26. CENOZOIC RADIOLARIANS FROM THE SOUTHWEST ATLANTIC, FALKLAND PLATEAU REGION, DEEP SEA DRILLING PROJECT LEG 71[1]

Fred M. Weaver,[2] Exxon Production Research Company, Houston, Texas

INTRODUCTION

Deep Sea Drilling Project Leg 71 occupied four sites and drilled six holes in the middle- to high-latitude regions of the southwest Atlantic Ocean. Sites 511 and 512 are located on the Falkland Plateau: 511 is at 51° 00.28′S, 46°58.30′W (2589 m water depth) in the plateau basin province and 512 at 49°52.19′S, 40° 50.71′W (1846 m water depth) on the northeastern margin of the Maurice Ewing Bank (Fig. 1). Sites 513 (47° 34.99S, 24°38.40′W; 4383 m water depth) and 514 (46° 02.76′, 26°51.29′W; 4318 m water depth) are positioned on the lower western flank of the Mid-Atlantic Ridge system. Hydraulic piston coring (HPC) was successfully used at Sites 512 and 514. Sediments were recovered at all the other sites using conventional coring methods.

As has been the case with previous DSDP Legs into the subantarctic and antarctic regions, bad weather and ice conditions considerably affected or delayed sediment coring, and we were unable to remain at several of the sites for as long as we would have preferred. However, we were very successful in recovering some heretofore uncollected high-latitude sections of Pliocene to Eocene age. The most interesting and scientifically productive intervals include (1) a composite, essentially complete, early Miocene to late Eocene section in Holes 511 and 513A; (2) an excellent middle/late Miocene boundary and middle Eocene section in Hole 512; (3) a very good late Miocene section containing sediments from Magnetic Chronozones 9, 6, and 5 in Hole 513A, and (4) a Pliocene interval with a high sedimentation rate in Hole 514 near the modern position of the Polar Front Zone. Detailed studies of these sections and other DSDP holes in subantarctic and antarctic regions significantly increase our understanding of Cenozoic and Mesozoic high-latitude biostratigraphy and paleoceanographic history.

Radiolarians are generally well preserved, abundant, and diverse in all Cenozoic sediments recovered during Leg 71. In contrast, the Mesozoic section collected at Hole 511 contains only a few sporadic occurrences of radiolarians in Samples 511-23,CC, 511-56,CC, and 511-57,CC. Most specimens are poorly preserved or recrystallized. Sample 511-23,CC contains a Maestrichtian assemblage with *Dictyomitra regina, D. lamellicostata*, and *Amphipyndax* sp., whereas Samples 511-56,CC and 511-57,CC yield specimens of the lower Albian to upper Aptian species *Thanarla conica* and *Archaeodictyomitra vulgaris*.

BIOSTRATIGRAPHIC FRAMEWORK

The antarctic/subantarctic radiolarian zonation proposed by Chen (1975) is used, with several modifications, to zone Neogene sediments recovered during Leg 71. Since a radiolarian zonation for the Paleogene has not been established in high latitudes and because most Paleogene species identified in Leg 71 samples are endemic to the area, Eocene and Oligocene age determinations are based on the occurrence of secondary marker species whose ranges are established in low-latitude regions (Riedel and Sanfilippo, 1978).

As part of the investigation of Leg 71 radiolarians, my data are supported by detailed radiolarian documentation from other DSDP sites and many *Eltanin* and *Islas Orcadas* piston cores from the Southern Ocean region. These include DSDP Leg 29, Hole 278; Leg 28, Hole 266; Leg 36, Hole 329; *Eltanin* Cores 16–4, 36–33, 50–28, 38–8, 14–8, 43–2, 13–17, and 34–5; and *Islas Orcadas* (IO) Cores 7–49, 7–54, 7–48, 7–55, 7–2, 16–108, and 16–109. Paleomagnetic data are available on these piston cores. Radiolarians in Holes 278, 266, and all *Eltanin* cores were documented in an earlier study (Weaver, 1976a). Detailed data from these cores will be published separately by Ciesielski and Weaver.

Piston cores provide a more complete record of early Pliocene radiolarian distribution throughout the Gilbert Magnetic Chronozone, thus allowing a high-resolution subdivision of Chen's (1975) *Helotholus vema* Zone into the *Desmospyris spongiosa, Triceraspyris coronata*, and *Stichocorys peregrina* zones. The *D. spongiosa* Zone is defined from the first occurrence of *D. spongiosa* to the evolutionary transition from *H. praevema* to *H. vema* (~4.25 to 4.0–3.95 Ma). The *T. coronata* Zone is defined from the last occurrence of *S. peregrina* to the first occurrence of *D. spongiosa* (~4.5 to 4.25 Ma). Finally, the *S. peregrina* Zone is defined by the total range of *S. peregrina* (~6.0 to 4.5 Ma). The base of the *S. peregrina* Zone is not directly correlated to paleomagnetic stratigraphy. However, in Hole 513A, the first occurrence of *S. peregrina* coincides with the first appearance of the diatom *Thalassiosira praeconvexa*, which in low latitudes correlates with the upper reversed interval of Chronozone 6 (Haq et al., 1980).

Radiolarian data from DSDP Leg 29, Hole 278, require a modification of Chen's (1975) late to middle Miocene zones. In Hole 278, *Antarctissa conradae* ranges below the first occurrence of *Actinomma tanyacan-*

[1] Ludwig, W. J., Krasheninnikov, V. A., et al., *Init. Repts. DSDP*, 71: Washington (U.S. Govt. Printing Office).

[2] Present address: Exxon U.S.A., Gulf/Atlantic Division, Houston, Texas.

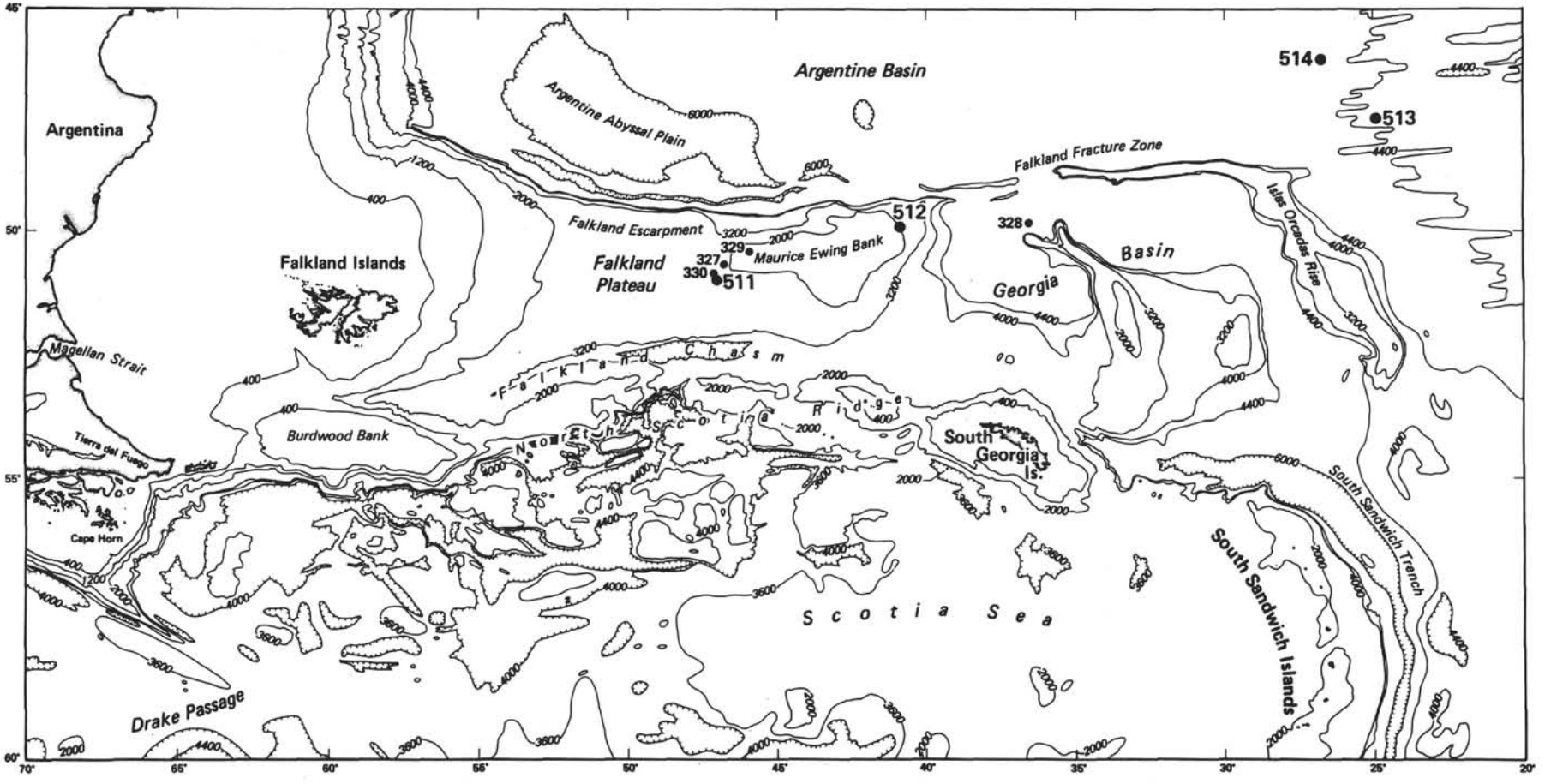

Figure 1. Location of Leg 71 sites.

tha (Petrushevskaya, 1975; this study). *Antarctissa conradae* has a split range that brackets the middle/late Miocene boundary. Therefore, I redefine Chen's (1975) *Actinomma tanyacantha* Zone from the first occurrence of *A. tanyacantha* to the first occurrence of *Theocalyptra bicornis spongothorax*, thus eliminating the *Antarctissa conradae* Zone. The top of the *Actinomma tanyacantha* Zone correlates with upper Magnetic Chronozone 10 or possibly basal 9 (~10.5 to 9.5 Ma) based upon data from Hole 512 and piston cores IO 7-55, 7-54, 7-49, and 7-48.

The *T. bicornis spongothorax* Zone of Chen (1975) is redefined from the first occurrence of *T. bicornis spongothorax* to the first occurrence of *S. peregrina* (~10.5-9.5 to 6.0 Ma). Piston core data from IO 7-49 shows that the upper range of *T. bicornis spongothorax* extends at least into Magnetic Chronozone 8 at ~8.3 Ma. As far as can be discerned, no upper Chronozone 8 to middle Chronozone 6 sections have been collected in piston cores from the Southern Ocean. This major gap in the sedimentary record spans the interval between 6.0 and 8.3 Ma.

Biostratigraphically Important Datums

Radiolarian stratigraphy in Neogene sediments from Leg 71 Holes 512, 513A, and 514 and the piston cores previously mentioned permits calibration of several Pliocene to middle Miocene datums to the geologic and paleomagnetic time scales. First-order correlations to paleomagnetic data are available for the Gauss, Gilbert, and Chronozones 11 through basal 8. Second-order correlations are used for the late Miocene interval between 6.1 and 5.4 Ma, where the occurrence of warm-water radiolarians and diatoms permits correlation with established low-latitude datum levels. These biostratigraphic events are:

1) First consistent occurrence (FCO) of *Cycladophora davisiana*, upper Gauss Chronozone, 2.8 to 2.6 Ma.

2) Morphotypic last occurrence (Tm) of *Prunopyle titan*, lower Gauss Chronozone, 3.2 Ma. Lower Gauss morphotypes of *P. titan* tend to be considerably smaller (average maximum width 150–180 μm) than those in the Gilbert, where the largest morphotypes occur between 4.0 and 4.25 Ma (average maximum width >210 μm).

3) Evolutionary transition of *Helotholus praevema* to *H. vema*, at or just below the Cochiti Subchronozone, ~3.95 Ma.

4) Morphotypic first occurrence (Bm) of *Lamprocyrtis heteroporos* and *Tholospyris* sp. A, upper Gilbert Chronozone, 3.95 Ma.

5) Tm of *Triceraspyris coronata*, just below the Nunivak Subchronozone, ~4.25 Ma.

6) Bm of *Desmospyris spongiosa*, below the Nunivak Subchronozone, 4.3 Ma.

7) Tm of *Amphymenium challengerae*, just above or within the Sidufjall Subchronozone, 4.35 Ma.

8) Tm of *Stichocorys peregrina*, within the lower Gilbert Chronozone, 4.6 to 4.4 Ma.

9) Tm of *Didymocyrtis didymus*, 5.4 Ma.

10) Tm of *Anthocyrtidium ehrenbergii* and Bm of *Amphymenium challengerae*, 5.45 Ma.

11) Tm of *Didymocyrtis* sp. A and *Lamprocyclas aegles* group, 5.5 Ma.

12) Bm of *Didymocyrtis didymus* and *Siphocampe* sp. A and the Tm of *Eucyrtidium* "spp.", ~5.6 Ma.

13) Bm of *Didymocyrtis* sp. A and *Lamprocyclas aegles* group, 6.0 to 5.8 Ma.

14) Bm of *Stichocorys peregrina*, ~6.0 Ma.

15) Tm of *Theocalyptra bicornis spongothorax*, 8.3 Ma. This is a maximum age for this datum. It is probably younger, but can only be tied with confidence to paleomagnetic stratigraphy up through basal Chronozone 8.

16) Tm of *Diartus hughesi*, top of Chronozone 9, at ~8.6 Ma.

17) Tm of *Actinomma tanyacantha*, probably within Chronozone 9, 9.5 to 9.8 Ma.

18) Bm of *Theocalyptra bicornis spongothorax*, basal Chronozone 9 to upper 10, 9.8 to 10.8 Ma.

19) Tm of *Cyrtocapsella japonica*, mid to basal Chronozone 10, 10.5 to 11.2 Ma.

Two points need to be emphasized concerning late Miocene to early Pliocene radiolarian stratigraphy. We do not have a very good understanding of lower Gilbert Magnetic Chronozone radiolarian distribution throughout the Southern Ocean (4.6 to 5.2 Ma). *Eltanin* Core 34-19, which is used by Keany (1979) to zone the lower Gilbert, is equivalent to a portion of Magnetic Chronozone 6, on the basis of data from Hole 513A. In addition, we also have very little documentation of radiolarian distributions for the interval between Magnetic Chronozones 8 and 6. A very detailed study of existing core material is under way to try to alleviate these inadequacies.

A preliminary middle Eocene through Oligocene radiolarian datum chart is being prepared from Leg 28, 29, 36, and 71 data. However, before it can be finished a considerable amount of taxonomic work remains to be completed. At least 60 new species are being described from Paleogene sediments recovered in Holes 511, 512, and 513A. These descriptions and the datum chart are being prepared for separate publication.

RADIOLARIAN HOLE SUMMARIES

Hole 511

Radiolarians are common and well preserved in Cores 1 through 20. Cores 21, 23, 56, and 57 contain rare recrystallized or poorly preserved radiolarians. All other cores are barren of siliceous microfossil remains.

Age Summary

In the absence of any well-documented high-latitude Paleogene radiolarian zonation, sediments recovered between Cores 2 and 20 are correlated with Riedel and Sanfilippo's (1978) standard low-latitude zonal scheme using rare secondary radiolarian indices. Table 1 illustrates the distribution and abundance of key radiolarian species identified in Hole 511.

Sample 511-1,CC contains a mixed assemblage of Quaternary, Pliocene, and Oligocene radiolarians indicating substantial disruption of sediments at this level. An unconformity spanning approximately 30 m.y. separates Cores 1 and 2.

Cores 2 through 4 are early Oligocene. They contain *Calocycletta* sp. cf. *C. parva*. This species is believed to be the ancestral form of *C. parva*, which appeared in the late Oligocene in low latitudes. Dinkelman (1973) reports that this species is restricted to the *Theocyrtis tuberosa* Zone, but Moore (1972) believes that it may range into the basal *Dorcadospyris ateuchus* Zone, or into the early late Oligocene. Therefore, Cores 2 through 4 are dated as early Oligocene to possibly early late Oligocene in age (Table 1).

Table 1. Radiolarians, Site 511.

Age	Radiolarian Zones	Core/Section (interval in cm)	Abundance	Preservation	*Antarctissa denticulata*	*Amphicraspedum prolixum*	*Amphymenium splendiarmatum*	*Buryella* sp.	*Calocyclas semipolita*	*Calocycletta acanthocephala*	*C.* sp. aff. *C. parva*	*Cryptoprora ornata*	*Cyclampterium? longiventer*	*C.?* sp. aff. *C. milowi*	*Diplocyclas* sp. A group	*Eucyrtidium* sp.	*Lithocyclia crux*	*Lithomelissa challengerae*	*L. sphaerocephalis*	*Lychnocanoma amphitrite*	*L.* sp. cf. *L. bellum*	*Spongothrochus glacialis*	*Theocalyptra davisiana*	*Theocyrtis diabloensis*	*T. tuberosa*	*Thrysocyrtis* sp. aff. *T. bromia*	*T.* sp. aff. *T. tetracantha*
	Mixed assemblage	1,CC	C	G	F				F				R			R							F	F			
	Theocyrtis tuberosa to early *Dorcadospyris ateuchus* zonal equivalent	2,CC	C	G					C		R		F	t		F		R	R								
		3,CC	C	G					C		R		C	F	t	F		R	R							R	
		4,CC	C	G					C	R	R		F	F	t	F			F							t	t
		5,CC	C	G					C	R			R	R	t	F		t	F							t	t
	T. tuberosa zonal equivalent	6,CC	C	G					C	t			F	t	t	F			R							t	t
		7,CC	C	G					C				F	R		R		t	R								
		8,CC	C	G					C	t			F	t	R	F		R	R							R	
		9,CC	C	G					C				F	t		F		t	R								
early Oligocene		10,CC											No recovery														
		11,CC	F	G					F					t		R											
		12,CC	C	G					C				R			F											t
		13,CC	C	G					C				t	R		t										t	
		14,CC											No recovery														
		15,CC											No recovery														
		16,CC	C	G					C	t				F	R	t										t	
late Eocene	*Thyrsocyrtis bromia* zonal equivalent	17,CC	C	G					C	F			t	R	R		R				t					t	t
		18,CC	C	G					C					R	R					t						R	t
		19,CC											No recovery														
		20,CC	C	G					C			t		F	F									R	t		
early-middle Eocene	Undifferentiated	21-1, 71-72	F	P		t	t	F																			

Note: For abundance, C = common, F = few, R = rare, t = trace (1–2 specimens/slide); for preservation, P = poor, M = moderately well preserved; G = good.

Cores 5 through 17 are dated as early Oligocene and are correlative to the *T. tuberosa* Zone in low latitudes. This correlation is based on the occurrence of *C. acanthocephala* throughout this sequence of cores. This species is known only from the early Oligocene or *T. tuberosa* Zone sediments in low- to middle-latitude regions. Johnson (1974) reports *C. acanthocephala* in *T. tuberosa* Zone sediments in the Indian Ocean and Ling (1975) documents its occurrence in the lower half of the *T. tuberosa* Zone in the Northwest Pacific area. (Core 17, however, is dated as latest Eocene on the basis of foraminiferal, calcareous nannofossil, and palynomorph data.)

Cores 18 to 20 are late Eocene in age and correlate with the *Thyrsocyrtis bromia* Zone in low latitudes. This age determination is based on the occurrence in these cores of *Cryptoprora ornata, Lychnocanoma amphitrite, Theocyrtis diabloensis*, and the ancestral form of *T. tuberosa*. Core 18 also contains very rare specimens of *Thyrsocyrtis bromia* and *T. tetracantha*.

Core 21 is tentatively dated as middle to early Eocene because of the co-occurrence of *Amphymenium splendiarmatum* and *Amphicraspedum prolixum* group along with many recrystallized specimens of *Buryella* species not identifiable to the specific level.

Paleoenvironmental Interpretation

The presence in Cores 16 through 20 of many specimens of *Calocycletta* and collosphaerid species along with specimens of *Cryptoprora ornata, Theocyrtis tuberosa* (ancestral form), *Lychnocanoma amphitrite, Lithocyclia crux*, and very rare *Thyrsocyrtis bromia* is indicative of relatively warm, possibly temperate conditions at Hole 511 during the latest Eocene and earliest Oligocene.

However, by Core 12 the specific nature of the overall radiolarian assemblage changes dramatically. Most warm-water species have disappeared and the assemblage becomes dominated by cooler water *Spongoplegma, Prunopyle*, and *Eucyrtidium* species. This assemblage persists through Core 11 and represents a significant climatic deterioration in the early Oligocene. Cores 11 and 12 appear to document the convergence of temperate and subantarctic waters after the transgression of subantarctic waters over Hole 511 in the early Oligocene.

Cores 2 through 9 contain radiolarians that resemble the early Oligocene assemblage recorded by Chen (1975) in Hole 274 at 60°S latitude near the Ross Sea. This assemblage is characterized by the occurrence of *Cyclam-*

pterium? longiventer, Calocyclas semipolita, Amphisphaera sp., *Diplocyclas* sp. A group, *Lithomelissa sphaerocephalis, L. challengerae, Spongomelissa* sp., and *Eucyrtidium* sp. (Table 1).

Chen (1975) records this assemblage in Cores 274-31 through 274-39. Because of their proximity to the Antarctic continent, these radiolarians are considered to be relatively cool-water species. Radiolarians in Cores 511-2 through 511-9 appear to represent the northerly elements of a broad antarctic/subantarctic biofacies that encompassed up to 18 degrees of latitude in the circum-Antarctic seas during the early Oligocene.

In summary, climatic conditions through the late Eocene to early Oligocene at Hole 511 fluctuate from temperate to at least subantarctic.

Holes 512 and 512A

Nineteen HPC cores were recovered at Hole 512 and one conventional core at Hole 512A. Very well preserved, abundant, and highly diverse radiolarians are encountered in all cores.

Miocene

Samples 512-1-1, 139–141 cm to 512-5,CC are correlated with the Miocene *Actinomma tanyacantha* Radiolarian Zone (Table 2). This interval spans the late/middle Miocene boundary, based upon foraminiferal data. The paleomagnetic stratigraphy of these sediments is interpreted by Ciesielski (this volume) to represent much of Chronozone 10 and the top of Chronozone 11 or the base of Chronozone 10 and most of Chronozone 11. However, without a more continuous section, it is impossible to say definitively which interpretation is correct.

The radiolarian assemblage encountered in Cores 512-1 through 512-5 is repetitious and is dominated by *Dendrospyris haysi, Prunopyle hayesi, Antarctissa conradae, Cornutella profunda, Theocalyptra bicornis, Eucyrtidium cienkowskii* group, and *Siphocampe arachnea* group. Less abundant species include *Cyrtopera laguncula, Actinomma tanyacantha, Lychnocanoma grande*, and *Gondwanaria japonica*. The only noticeable change in species composition occurs between Sections 512-3-2 and 512-2-2, where *Cyrtocapsella japonica* is documented (Table 2). The morphotypic top of *C. japonica* in low latitudes is within the *Diartus petterssoni* Zone (Johnson and Wick, 1982). They correlate this datum with the Chron 10/11 boundary at approximately 11.2 Ma.

The occurrence of many known deep-living radiolarian species such as *Cyrtopera laguncula, Cornutella profunda, Peripyramis circumtexta*, and *S. arachnea* group together with common to abundant *Thalassiothrix* spp. (diatom) throughout Cores 512-1 through 512-5 reflects eutrophic conditions. This association of diatoms and radiolarians is indicative of upwelling conditions (Weaver et al., 1981) and leads to the conclusion that Hole 512 was at or very near the Polar Front Zone between 11.5 and 10 Ma.

Eocene

Cores 512-6 through 512-19 and Core 512A-2 contain excellently preserved radiolarians dated as middle Eocene. No Paleogene zones exist at middle to high latitudes and no direct correlation to Riedel and Sanfilippo's (1978) low-latitude zonation is possible because of the paucity of stratigraphically important, low-latitude, index species. However, an indirect correlation is possible using secondary marker species such as *Eusyringium fistuligerum, E. lagena, Lithapium mitra*, and *Lophocyrtis biaurita* (Table 2).

Eusyringium fistuligerum, E. lagena, and *Lophocyrtis biaurita* range throughout Cores 512-6–19 and 512A-2 (Table 2). *Lithapium mitra* is found only in Cores 512-9 and 512-17. Based on radiolarian distributions at low latitudes, the highest occurrence of *L. biaurita* and the lowest occurrence of *L. mitra* are within the *Podocyrtis mitra* Zone. This interval is correlative with the NP15–NP16 nannofossil zones. While *E. fistuligerum* first occurs in low latitudes within the *Thyrsocyrtis triacantha* Zone, it co-occurs with *E. lagena* primarily within the *Podocyrtis ampla* to *P. mitra* zones. Therefore, based upon the occurrence of these secondary marker species, Cores 512-6–19 and 512A-2 are constrained to the *P. mitra* to *P. ampla* zones of Riedel and Sanfilippo, 1978 (Table 2).

The composite middle Eocene radiolarian assemblage at Holes 512 and 512A is dominated by *Cyclampterium?* sp. aff. *C. milowi, Lychnocanoma bellum, L.* sp. cf. *L. bellum, L. amphitrite, Periphaena decora, Theocotylissa* sp. aff. *T. ficus, Dictyoprora mongolfieri, Phormocrytis embolum, Lophocorys* sp. aff. *L. norvegiensis*, and *Lophocyrtis biaurita*. Numerous other new theoperid species were found within this interval and are now being described for publication.

Holes 513 and 513A

Radiolarians are common and well preserved throughout all cores recovered at Holes 513 and 513A. Ten cores were taken at Hole 513 and 33 at Hole 513A. Sediments range in age from Quaternary to early Oligocene.

Sample 513-1,CC contains a typical late Quaternary (<400,000 yr.) antarctic radiolarian assemblage that can be assigned to the *Antarctissa denticulata* Zone. Common species include *A. denticulata, A. strelkovi, Stylodictya validispina, Cycladophora davisiana, Lithelius nautiloides, Saccospyris antarctica*, and *Actinomma antarcticum*. The high abundance of *A. antarcticum* in this sample probably indicates proximity to the Polar Front Zone. Sample 513-3,CC is within the *Saturnalis circularis* Zone (approximately 0.7 to 1.6 Ma). This core catcher sample contains Quaternary radiolarians restricted to waters south of the Polar Front. Sample 513-4,CC is also in the *S. circularis* Zone, but it is below the morphotypic top of *Clathrocyclas bicornis* (1.6–1.8 Ma).

Sample 513-5,CC falls within the late Pliocene *Eucyrtidium calvertense* Zone (1.8–2.4 Ma). Typical late Pliocene antarctic radiolarians dominated by *Antarctissa denticulata* and *Spongotrochus glacialis* are present and indicate a position south of the Polar Front. The radiolarians in Sample 513-6,CC correlate to the upper part of the *Helotholus vema* Zone within the Gauss Magnetic Chronozone. No sediments were recovered from Cores 513-6–7. The early Pliocene *Triceraspyris coronata* Zone is represented in Samples 513-9,CC and 513-10,CC.

Table 2. Radiolarians, Holes 512 and 512A.

Age	Radiolarian Zones	Sample (interval in cm)	Abundance	Preservation	*Actinomma tanyacantha*	*Antarctissa conradae*	*Cornutella profunda*	*Cyrtocapsella japonica*	*Cyrtopera laguncula*	*Dendrospyris haysi*	*Eucyrtidium cienkowskii* group	*Gondwanaria japonica*	*Lychnocanoma grande*	*Peripyramis circumtexta*	*Prunopyle hayesi*	*Siphocampe arachnea* group	*Theocalyptra bicornis*	*Cyclampterium longiventer*	*C.* sp. aff. *C. milowi*	*Dictyprora mongolfieri*	*Eusyringium fistuligerum*	*E. lagena*	*Lithapium mitra*	*Lophocorys* sp. aff. *L. norvegiensis*	*Lophocyrtis biaurita*	*Lychnocanoma amphitrite*	*L. babylonis* group	*L. bellum*	*L.* sp. aff. *L. bellum*	*Periphaena decora*	*Phormocyrtis embolum*	*Phormocyrtis striata striata*	*Theocotylissa* sp. aff. *T. ficus*	*Thyrsocyrtis* sp. aff. *T. triacantha*
		Hole 512																															
late Miocene	*Actinomma tanyacantha* Zone	1-1, 137–139	F	G		F	F		t	R	t			t	R	F	R																
		1-2, 79–81	C	G	R	F	F		R	F	R	t	t	t	R	C	F																
		1,CC	C	G	F	F	R		t	F	R				F	C	F																
		2-1, 114–116	C	G	R	C	F		t	F	F	F	t	t	F	C	F																
		2-2, 99–101	C	G	t	F	F	R		F	F	F	t		R	C	F																
		2,CC	C	G		F	F	F		C	F	R	R	t	R	F	F																
		3-2, 76–78	C	G	t	C	F	R	t	F	F	R	R		F	C	F																
		3,CC	C	G	R	C	F			F	F				F	C	F																
middle Miocene		4-1, 59–61	F	G		C	R			F	F	t			F	C	R																
		4-2, 58–60	C	G	R	C	F			F	F	t			F	C	F																
		4,CC	C	G	R	F	F			F	R	t	t		R	C	F																
		5-1, 65–67	C	G	R	C	F			F	R				F	C	F																
		5-2, 74–76	F	G	R	C	F			F	F			t	R	C	F																
		5,CC	C	G	R	F	F			F	F	R	t		F	F	F																
		6-2, 10–12	C	G															F	F		R		F	F	R				R	R			
	Podocyrtis mitra zonal equivalent	6,CC	C	G														R	R	F	R			F	t	R	t		R	R	R		R	
		7-1, 105–107	C	M															F	F				F	R	R	R			R	R			
		7-3, 63–65	C	M															F	C		t		F	R	F	R			R		t		
		7,CC	C	G															F	R	R	R		F	R	R		t		F	t		R	
		8-1, 69–71	C	G															F	R		R		F	R	R				R	R			
		8,CC	C	G															F			R		F	R	R	R			R	R		R	
		9-1, 96–98	C	G															F	R				F	R	R				R	R		R	
		9-3, 64–66	C	G															F			R		F	R		R			F	R		R	
		9,CC	C	G															F	R	R		R	F	R	R	R			F	R		R	
		10-2, 32–34	C	G															F	R				F	R				R	R	R		R	
		10,CC	C	G															F	C	R	R		C	F	F	R		C	R	R	t	F	
		11-1, 78–80	C	G															F	C	R			C	F	F	R	R	R	R	F	R		
		11,CC	C	G															F	C	R	R		F	F	F	R	R	R	F	R	R	F	
middle Eocene		12-2, 58–60	F	G															F	R				C							R			
		12,CC	C	G															F	R		R		F	R	R		R	R	R	R		R	
		13-1, 33–35	C	G															F	R				R	F		R	R	R	F	R		R	
		13,CC	C	G															C	R		R		F	F	F	R	R	R	R	F		F	
		14-1, 68–70	F	M															F			R		R	R			R		R	F			
		14,CC	C	G															F			R		F	C	F	R	R		F	F	R	F	
		15-3, 15–17	C	G															F			R		F	C	R	R	R		F	F		R	
		15,CC	C	G															C		t	t		F	C	R	R	R	t	F	F		R	
		16-2, 19–21	C	G															C			R		R	F	R	R	R		F	F		R	
		16,CC	C	G															C	t	t	R		R	C	R	F	R	t	F	C	R	F	t
		17-3, 23–25	C	G															C	t		R	R	C	F	R	R	F		F	C		F	
		17,CC	C	G															C		t	t	R	C	C	R	F	R	R	F	F		F	t
	P. mitra to *P. ampla* zonal equivalent	18-2, 106–108	C	G															C					C	C	R	F	R		F	C		F	
		18,CC	C	G															C					C	C	F	F	F		R	F		F	
		19,CC	C	G															C	t	t	t		C	C	F	F	F		R	R		F	
		Hole 512A																																
		2,CC	C	G															C		t	t		C	C	R	F	F		F	F		F	t

Note: For abundance, C = common, F = few, R = rare, t = trace (1–2 specimens/slide), for preservation, P = poor, M = moderately well preserved; G = good.

Characteristic species include *T. coronata, H. praevema, C. bicornis, Eucyrtidium calvertense*, and *Stylatractus universus.*

Sample 513A-1,CC is assigned to the lower part of the early Pliocene *H. vema* Zone. Along with species typical of this zone (Chen, 1975) are found many warm-water species, including *Lamprocyclas maritalis, Dictyocoryne profunda/truncatum* group, *Tholospyris* sp. A, *Pterocanium trilobum, Lamprocyrtis heteroporos*, and many collosphaerids. Samples 513A-2,CC to 513A-4,CC are also early Pliocene and fall within the *Triceraspyris coronata* Zone (Table 3). *T. coronata* and *H. praevema*

are common constituents in Samples 513A-3,CC and 513A-4,CC. This interval is correlative with Samples 513-9,CC and 513-10,CC. The *Stichocorys peregrina* Zone is represented in Cores 513A-5 through 8. The Miocene/Pliocene boundary occurs within this zone at an apparent hiatus between Cores 4 and 5 (based on diatom data; Ciesielski, this volume). Diatom data further indicates that the interval between Section 513A-8-3 and 513A-5-5 correlates with upper Magnetic Chronozone 6 to lower Chronozone 5 (Ciesielski, this volume; Haq et al., 1980; Saito et al., 1975). Section 513A-8-4 Core 513A-6 is characterized by relatively warm water siliceous fauna and flora which allow a reliable correlation to low-latitude zonations. Warm-water radiolarians include *Anthocyrtidium ehrenbergii, Didymocyrtis didymus, D.* sp. A, *Lamprocyclas aegles* group, *Heliodiscus asteriscus*, and *Stichocorys peregrina* (Table 3). Radiolarians indicate that Hole 513A was situated north of the Polar Front between approximately 6.3 and 5.6 Ma.

A significant transition in the radiolarian fauna is observed between Cores 513A-6 and 5. In Core 5, most warm-water radiolarians have disappeared. Radiolarian abundances are greatly reduced and deeper-living forms such as *Siphocampe arachnea* group, *Cyrtopera laguncula, Cornutella profunda*, and *Peripyramis circumtexta* become progressively more dominant, especially between Sections 513A-5-4 and 513A-5-1. In contrast to Core 6, Core 5 contains a very high concentration of the diatom *Thalassiothrix* spp. This occurrence, together with the concentration of deep-living radiolarians, strongly suggests increased upwelling and very high productivity in the latest Miocene at Hole 513A. It further signals the late Miocene (~5.6–5.4 Ma) northward migration of the Polar Front to a position at or very near Hole 513A. This would be at least a degree or two north of its present position in the Southern Ocean today.

Very little sediment was recovered in Core 513A-9; however, Sample 513A-9,CC is tentatively dated as late Miocene, although it may be contaminated and unreliable for age analysis. Sections 513A-10-1 through 513A-11-1 fall within the *Theocalyptra bicornis spongothorax* Zone (Table 3). The last occurrence of *Diartus hughesi*

Table 3. Neogene radiolarians, Hole 513A.

Age	Radiolarian Zones	Core/Section (interval in cm)	Abundance	Preservation	*Amphymenium challengerae*	*Antarctissa conradae*	*A. denticulata*	*Anthocyrtidium ehrenbergi*	*Calocycletta* sp. aff. *C. caepa*	*Clathrocyclas bicornis*	Collosphaerids	*Cyrtocapsella cornuta*	*C. isopera*	*C. japonica*	*C. tetrapera*	*Dendrospyris haysi*	*Desmospyris spongiosa*	*Didymocyrtis* sp. A	*D. antepenultimus*	*D. didymus*	*D.* sp. aff. *D. didymus*	*Diartus hughesi*	*Eucyrtidium calvertense*	*E. cienkowskii* Group	*E. pseudoinflatum*	*Eucyrtidium* "spp."	*Gondwanaria japonica*	*Helotholus praevema*	*H. vema*	*Lamprocyclas aegles* group	*Lamprocyrtis hannai*	*L. heteroporos*	*Lithomelissa* sp. C	*Lychnocanoma grande*	*L. grande rugosum*	*L.* sp. aff. *L. grande*	*L. sphaerothorax*	*Prunopyle hayesi*	*P. titan*	*Sethophilium macropus*	*Theocalyptra bicornis*	*T. bicornis spongothorax*	*Theocorys redondoensis*	*Tholospyris* sp. A	*Triceraspyris coronata*	*Stichocorys peregrina*	*S. delmontensis*	*Siphocampe* sp. A
	Helotholus vema Zone	1,CC	C	G			F			C	R					t						C						R		F									C			
early Pliocene	*Triceraspyris coronatus* Zone	2,CC	C	G			F			F	R											F					C						t				F					F		
		3,CC	C	G			F			F												F					C													C			
		4,CC	C	G			R				R											F					C						R							C			
		5-1, 143–145	R	G	t	t																																						
		5-2, 143–145	C	G						R																	C			t													t	
		5-3, 73–75	C	G	C	t				F	F											R					C						R							F		F	t		
		5-4, 117–119	F	G	R					R												R					C															t		
		5-5, 143–145	C	G	F	R				F	R																C					t						t		R	R		
		5-6, 73–75	F	G	F					F																	C				t		R							R	R		
		5-7, 36–38	F	G	C					F	F											R					C						F							R		R			
		6-1, 143–145	C	G	C	t				F	F									R		F	R	R	t		C						C				R		R	R	C			
		6-2, 143–145	C	G	C	t				R	R									t		R					C						F							R	R			
		6-3, 73–75	C	G	R	F		t		F	R									C		F	R	t			C					t	R				R		F					F
	Stichocorys peregrina Zone	6-4, 73–75	C	G	C	R				F	F									R		F	R	t		R	C						F							R	F		t	
		6-5, 143–145	C	G		R		R		F	F									C		F	R	t		t	C					t	F				R		R	R	R	C	
		6-6, 73–75	C	M				R		F	F									F			R	t			C						R				R			t	t	F	
		6-7, 33–35	C	G		F				F	F							C					R	t	R	t	R		C	R			F			R			t	C	R	
		7-2, 61–63	C	G		R		R		F	F									F		R	R				F						F			R		R	R	F	F	
		7-3, 143–145	C	G		F				C	F							F					C	t	F		F						F			F			R	C		
		7-4, 143–145	C	G		R				F	R							R				t	F	R	F	t	R			F			R						t	C		
late Miocene		7-5, 73–75	C	G		F				F	F							F				R	F	t	R	R	F					R				R				C		
		7-6, 133–135	C	M		t		R		F	R							R				t	F		R	R	R						F	R			R				C		
		8-1, 28–30	C	G		F		R		F	R							F				t	C		F	R	C			F		t	R			R				C		
		8-2, 143–145	C	G				t		F	F											R	R		F	R	R					R	R		t	R			t	C		
		8-3, 73–75	R	G		t				R	F																R						t							R			
		8-4, 23–25	C	G		F		R		F	F											R	R	t	F		R						F	F		R		R		C	t		
		8-5, 143–145	F	M				F		R	F								t?				R				t						R	t			R				R		
		9-1, 72–74	C	M		R				R	F												t		R		t	t					R	F			R		t		R		
		9,CC	C	G		R		t		R	R												R	R	F													t		R			
		10-1, 17–19	F	G		R					F					t						R	R		R												R	R					
		10-2, 73–75	R	G							F												t														R						
	Theocalyptra bicornis spongothorax Zone	10-3, 73–75	C	G		R					C					R					F	t	F	t		R					R						R	R	R		t		
		10-4, 73–75	C	G		R					C										F	t	F	R		F						R	R				F	R		F	F		t	
		10-5, 73–75	C	G		F					C										F		F	R								R					R	R		R	R			
		10-6, 143–145	C	G							F										F		R	t		R											R	R		R			
		10-7, 12–13	F	G		F					F										F					R					t						R	R			t		
		10,CC	C	G							F					R					F		F	t														R					
		11-1, 36–38	C	G							F			t		R					F		F	R		R						R					R	t	R				
		11-2, 56–58	F	G							R			R		R												R										R					
		11-3, 143–145	C	G							F		R	R	F								C						R														
early Miocene	Undifferentiated	11,CC	C	G					R			R			F							F	F			R																R	
		12,CC	C	G							F	t		t	R								F					C										R					
		13,CC	C	G							R				R																							R					

Note: For abundance, C = common, F = few; R = rare; t = trace (1–2 specimens slide); for preservation, P = poor, M = moderately well preserved, preserved, G = good.

is in Section 513A-10-3 (Table 3). This datum occurs at the top of Chron 9 in low latitudes at approximately 8.6 Ma. (Johnson and Wick, 1982). A radiometric age determination on an ash layer in Section 513A-10-7 yields an age of 8.7 m.y. ±0.2 (Ciesielski, this volume). These data suggest that Core 513A-10 to Section 513A-11-1 correlates to the late Miocene Magnetic Chron 9. Section 513A-11-3 to Sample 513A-11,CC is middle to early Miocene, based upon the co-occurrence of *Cyrtocapsella cornuta* and *C. tetrapera*. Although the radiolarian assemblage is diverse and well preserved, neither low- nor high-latitude index species are present. Chen's (1975) and Riedel and Sanfilippo's (1978) zonations are not applicable. Cores 12 through 14 are early Miocene, based on silicoflagellate data. Radiolarians encountered in this interval are very diverse, as in Core 11, and correspondingly bear very little similarity to the early Miocene radiolarians known from low or high latitudes. Apparently these radiolarians represent a somewhat restricted early Miocene temperate biofacies. Radiolarians identified include *C. cornuta, C. tetrapera, Sethopilium macropus, Prunopyle hayesi, Lychnocanoma sphaerothorax, Lithomelissa* sp. C, *Eucyrtidium cienkowskii* group, and many species of collosphaerids. Many previously undefined species are being described from this interval.

Cores 513A-15 through 33 are dated as Oligocene. Radiolarians in these sediments are well preserved and very diverse but, as reported for the early Miocene assemblage, bear very little resemblance to low-latitude, time-equivalent faunas. Many undescribed species are present. Only four radiolarians reported from low-latitude sediments are observed within this interval: *Theocorys spongoconum, Artophormis gracilis*, and two species figured by Riedel and Sanfilippo (1977, plate 14, figs. 19–20, both listed as "theoperids gen. et sp. indet.").

A significant faunal change occurs between Cores 513A-28 and 27. Samples from Cores 28–33 correlate with Cores 511-2 through 6 or 7 on the Falkland Plateau. This stratigraphic overlap between Holes 511 and 513A provides an apparently complete Oligocene section situated in the cool temperate to subantarctic region of the Southwest Atlantic.

Hole 514

Quaternary to Pliocene radiolarians are present in all 35 HPC cores recovered at Hole 514. Abundance and diversity are high and preservation generally good. Hole 514 appears to be stratigraphically uninterrupted down to the Core 26/27 boundary, where an unconformity of approximately 700,000 yr. separates Gauss from upper Gilbert sediments.

Table 4 illustrates the occurrence and abundance of radiolarian species in Hole 514. Based on paleomagnetic stratigraphy, the Quaternary/Pliocene boundary occurs between Cores 4 and 5.

Core 514-1 falls within the *Antarctissa denticulata* Zone, Core 514-2 the *Stylatractus universus* Zone, Cores 514-3 through 5 the *Saturnalis circularis* Zone, Cores 514-6 to 10 the *Eucyrtidium calvertense* Zone and Cores 514-11 to 35 the *Helotholus vema* Zone (Table 4). Radiolarian zones and the range correlations of key species to the paleomagnetic time scale agree with the earlier data of Hays (1965) and Hays and Opdyke (1967).

Polar Front Migration

One of the primary objectives of Leg 71 was to collect a continuously cored late Cenozoic section near the modern position of the Antarctic Polar Front in order to document its evolution and migration through time.

Radiolarian assemblage analyses in Hole 514 record eight separate northward shifts in the Polar Front over this site during the Pliocene and Quaternary. These shifts are:

1) 3.9–4.0 Ma, Gilbert
2) 3.1 Ma, Gauss
3) 2.6–2.7 Ma, Gauss
4) 2.5 Ma, Gauss
5) 1.9–2.4 Ma, Matuyama
6) 1.9–2.4 Ma, Matuyama
7) 1.6 Ma, Matuyama
8) 0.4–0.7 Ma, Brunhes

Details of Polar Front migrations observed from radiolarians in Hole 514 are provided in Ciesielski and Weaver (this volume). Because of the major faunal reorganization at approximately 2.5 Ma (Hays and Opdyke, 1967), Polar Front history must be examined over two intervals, post-Gauss and pre-Matuyama. Post-Gauss Polar Front movements are documented by comparing downhole variations in radiolarian biofacies to their modern spatial distributions relative to the Polar Front Zone. Modern radiolarian biogeography is established using data from Hays (1965), Payne (1977), Nigrini (1967), Lozano and Hays (1976), Hays and Opdyke (1967), Petrushevskaya (1967), and Moore and Nigrini (1978). Latest Quaternary radiolarians indicative of waters north of the modern Polar Front include *Heliodiscus asteriscus, Pterocorys zancleus, Eucyrtidium acuminatum, Dictyocoryne profunda/truncatum* group, *Lamprocyclas maritalis*, and *Pterocanium praetextum eucolpum*. The biofacies restricted to the area near and south of Polar Front waters includes *Antarctissa denticulata, A. strelkovi, Saccospyris antarctica, Lithelius nautiloides, Triceraspyris antarctica*, and *Actinomma antarcticum*. Samples with significant numbers of *A. antarcticum* are presumed to record a position at or very near the Polar Front.

Identifying Polar Front movements in pre-Matuyama sediments presents a more difficult problem because of the increase in radiolarian species that are now extinct and about the paleoecology of which we know very little. However, detailed analyses of Pliocene radiolarian biogeography have identified several species with a restricted regional distribution that is almost certainly controlled by the position of the Pliocene Polar Front Zone. Data from Chen (1975), Weaver (1976a), Keany (1979), Hays and Opdyke (1967), and Hays (1965) are used to select those species.

Pre-Matuyama Pliocene radiolarians used to discern waters north of the Polar Front include *Lamprocyrtis heteroporos, Tholospyris* sp. A, *Lamprocyclas maritalis, Dictyocoryne profunda/truncatum* group, and col-

losphaerids (with very large pores). Species used to establish a position at or south of the Polar Front are *Desmospyris spongiosa, Helotholus vema, Antarctissa denticulata*, and *A. strelkovi*. The spatial distribution of these two radiolarian groups is similar to the two major radiolarian biofacies in modern antarctic and subantarctic waters.

LIST OF SPECIES

The following list provides a bibliography of references along with some observations of radiolarian taxa identified in Leg 71 sediments. In most cases the original author is cited along with an additional reference that contains information on the current concept of the species. Additionally, several new species are described and illustrated.

Actinomma antarcticum (Haeckel) Nigrini, 1967, p. 26, pl. 2, figs. 1a–d; Hays (1965), pp. 165–167, pl. 1, fig. 1.

Actinomma tanyacantha Chen, 1975, pp. 450–452, pl. 11, figs. 5–6. Plate 5, Figure 3.

Amphicraspedum prolixum Sanfilippo and Riedel, 1973, p. 524, pl. 10, figs. 7–11.

Amphirhopalum ypsilon Haeckel, 1887, p. 522; Nigrini, 1967, p. 35, pl. 3, figs. 3a–d.

Amphymenium challengerae n. sp. (Plate 6, Figures 1–2).

Description. Shell with two opposite segmented arms generally consisting of 4 to 5 distinct segments which are convex distally. Each arm segment penetrated by internal spines as basic framework; each segment covered by lattice work of circular to subcircular pores. Internal spines extend beyond shell segments as short projections. Arms arise from central structure composed of 2 inner spherical shells and 2 outer oblate spheroidal shells, all smooth and connected by numerous beams. In well-preserved specimens a patagium occurs around central structure and most chambered arm segments.

Measurements. Total length, 220–260 μm; length of arm, 75–95 μm; maximum width of arm, 90–105 μm; length of central structure, 85–100 μm; width, 75–95 μm. Measurements based on 25 specimens from 540 cm in *Eltanin* Core 16–4.

Abundance. Rare to common.

Occurrence. late Miocene to early Pliocene.

Type locality. E16–4, 540 cm.

Amphymenium splendiarmatum Clark and Campbell, 1942, p. 46, pl. 1, figs. 12, 14; Sanfilippo and Riedel, 1973, p. 524, pl. 11, figs 6–8; pl. 28, figs. 6–8.

Amphisphaera sp. Chen, 1975, p. 453, pl. 6, figs. 1–2.

Antarctissa conradae Chen, 1975, p. 457, pl. 17, figs. 1–5.

Antarctissa denticulata (Ehrenberg) Petrushevskaya, 1968, pp. 84–86, fig. 49, I–IV; Chen, 1975, p. 457, pl. 18, figs. 3–8. Plate 1, Figure 7.

Antarctissa strelkovi Petrushevskaya, (1968), pp. 88–90, fig. 51, III–VI.

Anthocyrtidium ehrenbergi (Stohr) Haeckel, 1887, p. 1277; Riedel, 1957, p. 83, pl. 20, figs. 1–9. Plate 4, Figure 6.

Artophormis gracilis Riedel, 1959, p. 300, pl. 2, figs. 12–13; Moore, 1971, p. 742, pl. 5, figs. 10–11.

Botryostrobus miralestensis (Campbell and Clark) Petrushevskaya and Kozlova, 1972, p. 539, pl. 24, fig. 31; Nigrini, 1977, p. 249, pl. 1, fig. 9.

Buryella sp. Recrystallized specimens not recognized to the species level.

Calocyclas semipolita Clark and Campbell, 1942, p. 83, pl. 8, figs. 12, 14, 17–19, 21–23; Chen, 1975, p. 459, pl. 6, figs. 3–6.

Calocycletta acanthocephala (Ehrenberg) Petrushevskaya and Kozlova, 1972, p. 544, pl. 35, figs. 5–7; Johnson, 1974, p. 550, pl. 6, fig. 3.

Calocycletta sp. cf. *C. parva* Dinkelman, 1973, pl. 7, fig. 3.

Calocycletta sp. aff. *C. caepa* Moore, 1972.

Clathrocyclas bicornis Hays, 1965, p. 179, pl. 3, fig. 3; Chen, 1975, p. 489, pl. 12, figs. 8–9. Plate 2, Figure 5.

Collosphaera sp.

Cornutella profunda Ehrenberg, 1858, p. 31; Riedel, 1958, p. 232, pl. 3, figs. 1–2. Plate 1, Figure 6.

Cyrtoprora ornata Ehrenberg, 1874, p. 222; Riedel and Sanfilippo, 1971, pl. 3D, figs. 10–11; Sanfilippo and Riedel, 1973, p. 530, pl. 35, figs. 3–4.

Cycladophora davisiana Ehrenberg, 1862, p. 297; Riedel, 1958, p. 239, pl. 4, figs. 2–3; Weaver, 1976a, p. 581, pl. 1, fig. 7. Plate 1, Figure 3.

Cyclampterium? longiventer Chen, 1975, pp. 459–460, pl. 10, fig. 7.

Cyclampterium? sp. aff. *C. milowi* Riedel and Sanfilippo, 1971. Specimens have a very large inflated abdomen with large pores similar to *C. milowi*, but lack the well-developed latticed feet.

Cyrtocapsella cornuta (Haeckel) Riedel and Sanfilippo, 1978, p. 68, pl. 4, fig. 17.

Cyrtocapsella isopera Chen, 1975, p. 460, pl. 11, figs. 7–9; Weaver, 1976a, p. 581, pl. 3, figs. 5–6; pl. 9, figs. 4, 6.

Cyrtocapsella japonica (Nakaseko) Sanfilippo and Riedel, 1970, p. 452, pl. 1, figs. 13–15; Kling, 1973, p. 636, pl. 11, figs. 19–20.

Cyrtocapsella tetrapera (Haeckel) Riedel and Sanfilippo, 1978, p. 68, pl. 4, fig. 18; Weaver, 1976a, p. 581, pl. 3, figs. 1–3; pl. 9, figs. 1–3, 7. Plate 6, Figure 4.

Cyrtopera laguncula Haeckel, 1887, p. 1451, pl. 75. fig. 10; Chen, 1975, p. 460, pl. 18, fig. 9.

Dendrospyris haysi Chen, 1975, p. 455, pl. 15, figs. 3–5; Weaver, 1976a, p. 579, pl. 2, figs. 7–9; pl. 7, fig. 4. Plate 5, Figure 4.

Desmospyris spongiosa Hays, 1965, pp. 173–175, pl. 2, fig. 1; Weaver, 1976a, p. 579, pl. 1, fig. 12; Chen, 1975, p. 456, pl. 15, figs. 1–2. Plate 2, Figures 6–8.

Dictyocoryne profunda/truncatum group Ehrenberg, 1872, p. 307, pl. 7, fig. 23.

Dictyoprora mongolfieri (Ehrenberg) Nigrini, 1977, pp. 250–251, pl. 4, fig. 7; Riedel and Sanfilippo, 1978, p. 76, pl. 9, fig. 13.

Didymocyrtis sp. A. Similar to *Ommatartus* sp. A Foreman, 1975, p. 618, pl. 8, figs. 20–23, but much more heavily silicified. Plate 6, Figure 5.

Didymocyrtis antepenultimus (= *Ommatartus antepenultimus*) Riedel and Sanfilippo, 1978, p. 71, pl. 7, fig. 6. Plate 5, Figure 2.

Didymocyrtis didymus Ehrenberg, 1844, p. 83; Riedel et al., 1974, p. 706, pl. 55, figs. 3–5; Zachariasse et al., 1978, p. 105, pl. 2, figs. 10–11. High-latitude forms of this *Didymocyrtis* species encountered in Hole 513A sediments are similar to those referred to as *Ommatartus didymus* by Riedel et al., 1974. These forms have large multiple polar caps. Sanfilippo et al., 1973, have suggested that *D. didymus* is a cold-water form of *Diartus hughesi*. If this is true, then *Didymocyrtis didymus* persisted at high latitudes for a considerable time after *Diartus hughesi* became extinct in low-latitude regions. Plate 6, Figures 7–8.

Didymocyrtis sp. aff. *D. didymus* (Ehrenberg, 1844).

Diartus hughesi (= *Ommatartus hughesi*) (Campbell and Clark) Riedel and Sanfilippo, 1978, p. 71, pl. 7, fig. 7. Plate 5, Figure 1.

Diplocyclas sp. A group Chen, 1975, p. 460, pl. 7, figs. 4–5.

Eucyrtidium acuminatum Ehrenberg, 1844, p. 84; Nigrini, 1967, p. 81, pl. 8, figs. 3A, B.

Eucyrtidium calvertense Martin, 1904, p. 450, pl. 130, fig. 5; Hays, 1965, p. 181, pl. 3, fig. 4; Weaver, 1976a, p. 581. pl. 1, fig. 9. Plate 2, Figure 9; Plate 4, Figure 7.

Eucyrtidium cienkowskii group Haeckel, 1887, p. 1493, pl. 80, fig. 9; Weaver, 1976a, p. 581, pl. 4, figs. 3–5; pl. 8, figs. 7–9. Plate 5, Figure 6.

Eucyrtidium pseudoinflatum n. sp. (Plate 5, Figures 8–9).

Description. Shell truncate fusiform, inflated; abdomen and postabdominal segments are marked or separated by internal septa. Cephalis spherical, partially sunken into the thorax. Contains a few small, circular pores. Collar stricture generally slight or indistinct. Thorax inverted conical with 4–5 rows of small pores arranged in desicussate rows. Lumbar stricture marked by distinct change in contour. Abdominal segment contains 7–8 longitudinal furrows in which lie circular pores approximately twice the size of the thoracic pores. Shell reaches maximum width within this segment. First postabdominal segment truncate conical, approximately half the length of the abdomen; contains an equal number of furrows, and pores of a smaller diameter. In well-preserved specimens there is a second postabdominal segment that is truncate conical and contains only a few small, irregularly spaced pores.

Discussion. *E. pseudoinflatum* resembles *E. inflatum* Kling, 1973, in its overall size and inflated appearance. However, it differs

Table 4. Radiolarians, Site 514.

Age	m.y.	Magnetic Polarity Zone	Core/Section	Abundance	Preservation	*Actinomma antarcticum*	*Amphirhopalum ypsilon*	*Antarctissa denticulata*	*A. strelkovi*	*Botryostrobus miralestense*	*Clathrocyclas bicornis*	*Collosphaera* sp.	*Cornutella profunda*	*Cycladophora davisiana*	*Desmospyris spongiosa*	*Dictyocoryne profunda/truncatum* group	*Eucyrtidium acuminatum*	*E. calvertense*	*Gondwanaria* sp.	*Heliodiscus asteriscus*	*Helotholus vema*
Quaternary	0.72	Brunhes	1,CC	C	M	F		C					R	F			F			R	
			2,CC	C	G	F		C	F				R	F							
	0.91		3,CC	C	G	F	t	F		R			R	F		R	F				
	0.98		4,CC	C	G	F/C		C	R	F			R	F							
	1.66		5,CC	C	G	C		C	F		F		R	F							
	1.88	Matuyama	6,CC	C	G	C		C	F		F		F	F		R	R	t			
			7,CC	C	G	F		C			F		F			F		F			
			8,CC	C	G	F		C			F			F				F			
			9,CC	C	G			F	F	R	F		F	R				F			
			10,CC	C	G	C		C			F		F	R				F			
Pliocene	2.47	Gauss	11,CC	C	G			C			F		F	R	R			F			C
			12,CC	C	G			F	F		F		F		F			F			F
			13,CC	C	G			F			F		R		F	R		F			F
			14,CC	C	G			F			F		F		F			F			F
			15,CC	C	G			F			F		F		F	F		F	R		F
			16,CC	C	G			C			F		F		F	F		R			F
			18,CC	C	G			C			F		F		t	R		F	F		R
			19,CC	C	G			F			F		F		t	F		F	F		R
			20,CC	C	G			F			F		F		t	F		F	F		
	2.92		21,CC	C	M			F			F		R		t	F		F			t
	2.99		22,CC	C	G			F			F		F		t	F		F			t
			23,CC	C	G			F			F		F		R	F		F			F
	3.08		24,CC	C	G			F			F	R	R		t	F		F	F		t
			25,CC	C	G			F			F		F			F		F	F		t
			26,CC	C	G			C			F		F		R			F	R		F
	3.86		27,CC	C	G			F			F		R		R	F		F	t		R
			28,CC	C	G			F			F		F			F		F	R		t
	3.95		29,CC	C	G			F			F		R			F		F	t		F
			30,CC	C	G			F	F		F		F		F			F			F
		Gilbert	31,CC	C	G			F			F		F		t	F		F		t	t
			32,CC	C	M			F			F		F		t	F		F	t		t
			33,CC	C	G						C		F					C	F		
			34,CC	C	G			F			F		F			F		F	R		t
			35,CC	C	G			R			F				t	F		F			t

Note: For abundance, C = common, F = few, R = rare, t = trace (1–2 specimens/slide); for preservation, P = poor M = moderately well preserved, G = good.

from *E. inflatum* in having a greater number of longitudinal furrows, smaller pore diameter, and a maximum width which is attained in the mid to upper first abdominal segment. *E. inflatum* Kling attains a maximum width in the lowermost abdomen or at the division of the abdomen and fourth segment.

Measurements. Total length of shell, 145–175 μm; cephalis, 15–22 μm; thorax, 30–38 μm; abdomen, 50–75 μm; all postabdominal segments, 35–52 μm; maximum shell width, 90–110 μm; diameter of pores, 2–6 μm. Measurements based on 25 specimens from DSDP Samples 278-10-2, 43–45 cm, 278-10-3, 48–50 cm, and 278-10-4, 54–56 cm.

Abundance. rare to few.

Occurrence. late Miocene.

Type locality. DSDP Sample 278-10-3, 48–50 cm.

Holotype. Plate 5, Figures 8–9.

Eusyringium fistuligerum (Ehrenberg) Riedel and Sanfilippo, 1978, p. 68, pl. 5, figs. 6–7.

Eusyringium lagena (Ehrenberg) Riedel and Sanfilippo, 1978, p. 68, pl. 5, fig. 8.

Eucyrtidium sp. Chen, 1975, p. 461, pl. 7, figs. 6–8.

Eucyrtidium "spp." Sanfilippo and Riedel, 1970, p. 450, fig. 1.

Gondwanaria japonica (Nakaseko) Petrushevskaya, 1975, p. 584, pl. 8, fig. 15; pl. 9, figs. 2–7; pl. 12, fig. 1.

Gondwanaria sp.

Table 4. (Continued).

Lamprocyclas maritalis	*Lamprocyrtis hannai*	*L. heteroporos*	*Lithelius nautiloides*	*Lychnocanoma grande rugosum*	*Peripyramis circumtexta*	*Polysolenia* sp.	*Prunopyle titan*	*Pterocanium praetextum eucolpum*	*P. trilobum*	*Pterocorys hirundo*	*P. zancleus*	*Saccospyris antarctica*	*S. conithorax*	*S. praeantarctica*	*Saturnalis circularis*	*Spongothrochus glacialis*	*Spongurus pylomaticus*	*Stichoplium* sp.	*Stylatractus neptunus*	*S. universus*	*Theocalyptra bicornis*	*Tholospyris* sp. A	*Triceraspyris antarctica*	Radiolarian Zones
	R		R		R						R	F	F		t	F					F		F	*Antarctissa denticulata* Zone
R			R		R							F	F			F	F			t	F		F	*Stylatractus universus* Zone
			R		R			R	R		F	F	F		F	F	F				F		F	*Saturnalis circularis* Zone
			R		R			F	F			F			F	F	F		R	F			F	
			R			R			R			F	F		R	F	F		R				F	
											F	F			F	F			R	R			F	
F						F						F			F	F							F	*Eucyrtidium calvertense* Zone
															F	F							F	
R			R							F			F		R	F			R					
		R			R					F					R	F								
		F			R										F	F				R				
										F					F	F								
F		F													R	F				R				
t			F		R									F	R	F				R			R	
t		F								F				R	R	F			F	R		t		
R		F	R		R										R	F				R		F		
F		F								F			R		F	F				F		C		
F		F			R	R									F	F						C		
F		F			R										F	F				F		C		
R		t			R	R				t			t	R	F	F				R		C		
		F			R					F		R			F	C				F		F		
		R		t	R					R			t		F	F				F		F		
		F		t											F	F		R		F		F		*Helotholus vema* Zone
F		R		t		R			t				t		F	R						F		
R		t		t	R	R									F	F		R				R		
R		F	t	t			F			F					F	F				t		F		
F		F				R	F								R	F		R				F		
R		F		t	R		F							t	R	F				t		F		
					F		F							R	F	F			F	F				
F		F				R	R	F	t			F			R	R		R				F		
R		R					F									F		R		R		F		
F		F				R	R								R	F				R		C		
t		F			F	F	F								R	F						F		
R		F					F									F		F				F		

Heliodiscus asteriscus Haeckel, 1887, p. 455, pl. 33, fig. 8; Hays, 1965, p. 171, pl. 2, fig. 7.

Helotholus praevema n. sp. (Plate 3, Figs. 1, 5–15).

Description. Shell consists of two segments. Cephalis spherical, with numerous circular to subcircular pores and 1 or 2 apical spines. Cephalis width, one-half to two-thirds thorax. Collar stricture is distinct. Thorax variable, predominantly subcylindrical, sometimes cup-shaped, with numerous circular to elliptical pores. Commonly pores are irregularly spaced or exhibit crude longitudinal alignment. In well-preserved specimens, supplementary spines protrude from thoracic wall as apparent extensions of the internal structure. Internal structure consists of the elements A, D, V, Lr, and L1 spines, all arising from a common point in plane of collor stricture. An axial spine (Ax) projects downward into thoracic cavity from this point. No distinct median bar (Mb) observed; point of convergence of internal spines could be perceived as short Mb. Where primary interval spines are fused to thoracic wall, it is drawn into shell, forming grooves on surface.

Discussion. The internal structure of *Helotholus praevema* closely resembles that of *H. histricosa* Jorgensen. *H. praevema* might become confused with *Antarctissa strelkovi*, but it differs from this species in having a distinct collar stricture. The internal structure also differs from *A. strelkovi* and *H. histricosa* sensu Riedel, 1958, in that these species have a distinct Mb (see fig. 51.6, Petrushevskaya, 1967, p. 89, and Riedel, 1958, p. 235, figs. 6–7). *H. praevema* evolved to *H. vema* just prior to the Cochiti Subchron. This species transition during the early Pliocene involves (1) almost two fold increase in thoracic width, (2) a gradual invagination of the cephalis into the thorax (Kellogg, 1975), (3) the formation of up to 12 large subcircular to elliptical pores on the flat

horizontal portion of the upper thorax, and (4) a transformation of the internal structure by the development of a basal ring and several horizontal and oblique beams that connect it to the thoracic wall. Kellogg (1975) considered *H. praevema* and *H. vema* to be the same species, and documented this evolutionary transition as directional selection for larger phenotypes of the same species. Just prior to the evolutionary transition of *H. praevema* to *H. vema*, the cephalis became slightly invaginated into the thorax, and some specimens could become confused with *A. strelkovi*. Examination of the internal structure, however, would prove definitive.

Measurements. Length of shell, 90–160 μm; cephalis, 38-55 μm; maximum width of thorax, 70–135 μm. Measurements based on 100 specimens from *Eltanin* Core E 50–28, 411 cm, 380 cm; Core E 38–8, 460 cm, 480 cm, and 540 cm.

Abundance. rare to common.

Range. late Miocene to early Pliocene.

Type locality. E 38–8, 500 cm.

Holotype. Plate 3, Figure 9.

Helotholus vema Hays, 1965, p. 176, pl. 2, fig. 3; Chen, 1975, p. 457, pl. 16, figs. 1–4; Weaver, 1976a, p. 580, pl. 1, figs. 10–11. Plate 3, Figures 2–4.

Lamprocyclas aegles group (Ehrenberg) Petrushevskaya and Kozlova, 1972, p. 544, pl. 36, fig. 13. Plate 4, Figures 4–5.

Lamprocyclas maritalis Haeckel; Nigrini, 1967, p. 74, pl. 7, fig. 5. Plate 4, Figure 8.

Lamprocyrtis hannai (Campbell and Clark) Kling, 1973, p. 638, pl. 5, figs. 12–14; pl. 12, figs. 10–14.

Lamprocyrtis heteroporos (Hays) Kling, 1973, p. 639, pl. 5, figs. 19–21; pl. 15, fig. 6. Plate 4, Figure 1.

Lithapium mitra (Ehrenberg) Riedel and Sanfilippo, 1978, p. 69, pl. 6, figs. 1–2.

Lithelius nautiloides Popofsky; Chen, 1975, p. 455, pl. 24, fig. 7.

Lithocyclia crux Moore; Riedel and Sanfilippo, 1978, p. 70, pl. 6, fig. 7.

Lithomelissa challengerae Chen, 1975, p. 457, pl. 8, fig. 3.

Lithomelissa sphaerocephalis Chen, 1975 p. 457, pl. 8, figs. 1–2.

Lithomelissa sp. *C.* Chen, 1975, p. 458, pl. 11, figs. 3–4. Plate 5, Figure 5.

Lophocyrtis biaurita (Ehrenberg) Riedel and Sanfilippo, 1978, p. 70, pl. 6, fig. 13.

Lophocorys sp. aff. *L. norvegiensis* Bjørklund and Kellogg, 1972.

Lychnocanoma amphitrite Foreman, 1973, p. 437, pl. 11, fig. 10; Riedel and Sanfilippo, 1978, p. 70, pl. 7, figs. 2–3.

Lychnocanoma babylonis group (Clark and Campbell) Riedel and Sanfilippo, 1970, p. 528, pl. 9, figs. 1–3.

Lychnocanoma bellum (Clark and Campbell) Riedel and Sanfilippo, 1970, p. 529, pl. 10, fig. 5; Foreman, 1973, p. 437, pl. 1, fig. 17; pl. 11, fig. 9.

Lychnocanoma sp. aff. *L. bellum* (Clark and Campbell, 1942).

Lychnocanoma grande (Campbell and Clark) Kling, 1973, p. 637, pl. 10, figs. 11, 13–14; Weaver et al., 1981, p. 82, pl. 2, figs. 4–5.

Lychnocanoma grande rugosum (Riedel), 1952, pl. 6, fig. 1; Hays, 1965, p. 175, pl. 3, fig. 5.; Weaver 1976a, p. 581, pl. 9, fig. 5. Plate 2, Figure 1.

Lychnocanoma sp. aff. *L. grande* (Campbell and Clark, 1944).

Lychnocanoma sphaerothorax Weaver, 1976, pp. 581–582, pl. 5, figs. 4–5.

Periphaena decora Ehrenberg; Sanfilippo and Riedel, 1973, pl. 8, figs. 8–10; pl. 27, figs. 2–5.

Peripyramis circumtexta Haeckel, 1887, p. 54, fig. 5; Weaver, 1976a, p. 582, pl. 1, fig. 5. Plate 1, Figure 1.

Phormocyrtis embolum (Ehrenberg) Johnson, 1974, p. 548, pl. 4, fig. 5.

Phormocyrtis striata striata Brandt; Riedel and Sanfilippo, 1978, p. 71, pl. 7, fig. 11.

Polysolenia sp.

Prunopyle hayesi Chen, 1975, p. 454, pl. 9, figs. 3–5; Weaver, 1976a, p. 578, pl. 7, figs. 1–3.

Prunopyle titan (Campbell and Clark) Hays (1965), p. 173, pl. 2, fig. 4; Weaver, 1976a, p. 578, pl. 7, fig. 6.

Pterocanium praetextum eucolpum Haeckel; Moore and Nigrini, 1979, pp. N43–N44, pl. 23, fig. 3.

Pterocanium trilobum (Haeckel) Moore and Nigrini, 1979, pp. N45–N46, pl. 23, figs. 4a–c.

Pterocorys hirundo Haeckel, 1887, p. 1318, pl. 71, fig. 4; Riedel, 1958, p. 238, pl. 4, fig. 1; Chen, 1975, p. 458, pl. 19, fig. 3.

Pterocorys zancleus (Müller) Moore and Nigrini, 1979, pp. N89–N90, pl. 25, figs. 11a–b.

Saccospyris antarctica Haeckel; Weaver, 1976a, p. 582, pl. 1, fig. 6; Petrushevskaya, 1968, pp. 149–150, fig. 85, 11. Plate 1, Figure 4.

Saccospyris conithorax Petrushevskaya, 1965, pp. 98–99, fig. 11; 1968, p. 150, fig. 85, 1.

Saccospyris praeantarctica Petrushevskaya, 1975, p. 589, pl. 13, figs. 19–20. Plate 1, Figure 8.

Saturnalis circularis Haeckel; Chen, 1975, p. 454, pl. 24, fig. 2; Weaver, 1976a, p. 579, pl. 1, fig. 4. Plate 1, Figure 5.

Sethopilium macropus Haeckel; Riedel and Sanfilippo, 1977, pl. 15, fig. 11.

Siphocampe arachnea group (Ehrenberg) Nigrini, 1977, p. 255, pl. 3, figs. 7–8.

Siphocampe sp. A. Shell thick-walled, robust, consists of 4 segments of which 3rd or 4th is the broadest. Cephalis approximately spherical with lateral tubule that curves slightly downward and lies along thorax. The cephalis contains numerous circular to subcircular pores. Thorax short, truncate conical, with 2–3 rows of circular pores arranged approximately in transverse rows. Lumbar and postlumbar strictures are slight. Abdomen nearly cylindrical with small circular pores arranged in 4 to 5 transverse rows. First postabdominal segment may be slightly inflated, pores circular and arranged in 3–5 transverse rows. This segment tapers distally to terminate in very distinct poreless peristome. The thoracic and abdominal pores commonly appear deepset and tilted downward. Total length, 120–135 μm. Length of cephalis, 11-20 μm; thorax, 20–25 μm; abdomen, 80-90 μm. Maximum width, 70–80 μm. Plate 4, Figure 9; Plate 6, Figure 6.

Spongothrochus glacialis Popofsky; Chen, 1975, p. 455, pl. 24, figs. 5–6.

Spongomelissa sp. Chen, 1975, p. 458, pl. 10, fig. 4.

Spongurus pylomaticus Riedel, 1958, p. 226, pl. 1, figs. 10–11; Moore and Nigrini, 1979, pp. S65–S66, pl. 8, figs. 3a–b.

Stichocorys delmontensis (Campbell and Clark) Sanfilippo and Riedel, 1970, p. 451, pl. 1, fig. 9; Kling, 1973, p. 638, pl. 11, figs. 8–10.

Stichocorys peregrina (Riedel) Sanfilippo and Riedel, 1970, p. 451, pl. 1, fig. 10; Weaver et al., 1981, p. 83, pl. 4, figs. 1–2. Plate 6, Figures 3, 9.

Stichopilium sp.

Stylodictya validispina Jorgensen; Petrushevskaya, 1968, p. 30, pl. 17, figs. 4–5. Plate 1, Figure 9.

Stylatractus neptunus Haeckel, 1887, p. 328, pl. 17, fig. 6; Riedel, 1958, p. 226, pl. 1, fig. 9.

Stylatractus universus Hays, 1965, p. 167, pl. 1, fig. 6; 1970, p. 215, pl. 1, fig. 1.

Theocalyptra bicornis Popofsky; Chen, 1975, p. 462, pl. 13, figs. 1–2.

Theocalyptra bicornis spongothorax Chen, 1975, p. 462, pl. 12, figs. 1–3; Weaver, 1976a, p. 582, pl. 2, figs. 1–4; pl. 6, figs. 2–4. Plate 5, Figure 7.

Theocorys spongoconus Kling, 1971, p. 1087, pl. 5, fig. 6; Riedel and Sanfilippo (1978), p. 76, pl. 9, fig. 16.

Theocorys redondoensis (Campbell and Clark) Kling, 1973, p. 638, pl. 11, figs. 26–28; Weaver et al., 1981, p. 82, pl. 2, figs. 1–2. Plate 2, Figure 4.

Theocotylissa sp. aff. *T. ficus* (Ehrenberg, 1873).

Theocyrtis diabloensis Clark and Campbell, 1942, p. 90, fig. 13; Chen, 1975, p. 459, pl. 5, figs. 4–7.

Theocyrtis tuberosa Riedel, 1959, p. 298, pl. 2, figs. 10–11; Riedel and Sanfilippo, 1978, p. 78, pl. 1, fig. 10. The specimens of *T. tuberosa* identified in Hole 511 are similar to the ancestral form of the species.

Tholospyris sp. A. Lattice shell crown-shaped; sagittal stricture slight. Apical spine short, often broken. Sagittal ring appears to be D-shaped; joined to front, apex, and back of the shell. Lattice shell smooth, constricted along sagittal ring; perforated by small circular to subcircular, closely spaced lattice pores. Three short bladed feet, broad and fenestrated proximally, tapering quickly,

distally. In some specimens, lattice shell extends below base and joins proximal ends of feet. Latticework between the feet contains numerous pores of irregular size and shape. Maximum width, 85–114 μm; maximum length, 70–96 μm; length of feet, 20–33 μm. Plate 4, Figures 2–3.

Thyrsocyrtis sp. aff. *T. bromia* (Ehrenberg, 1873).

Thyrsocyrtis sp. aff. *T. tetracantha* (Ehrenberg, 1873).

Thyrsocyrtis sp. aff. *T. triacantha* (Ehrenberg, 1873).

Triceraspyris antarctica (Haeckel) Weaver (1976), p. 579, pl. 1, figs. 2–3. Plate 1, Figure 2.

Triceraspyris coronata Weaver, 1976, p. 580, pl. 2, figs. 4–5; pl. 6, figs. 8–9. Plate 2, Figures 2–3.

REFERENCES

Bandy, O. L., Casey, R. E., and Wright, R. C., 1971. Late Neogene planktonic zonation, magnetic reversals, and radiometric dates, Antarctic to the Tropics. *In* Reid, J. L. (Ed.), *Antarctic Oceanology I.* Am. Geophys. Union, Antarct. Res. Ser., 15:1–26.

Bjørklund, K. R., 1976. Radiolaria from the Norwegian Sea, Leg 38 of the Deep Sea Drilling Project. *In* Talwani, M., Udintsev, G., et al., *Init. Repts. DSDP,* 38: Washington (U.S. Govt. Printing Office), 1101–1168.

Bjørklund, K. R., and Kellogg, D. E., 1972. Five new Eocene radiolarian species from the Norwegian Sea. *Micropaleontology*, 18: 386–396.

Campbell, A. S., and Clark, B. L., 1944. *Miocene Radiolarian Faunas from Southern California.* Geol. Soc. Am. Spec. Paper 51.

Chen, P.-H. 1975. Antarctic radiolaria. *In* Hayes, D. E., Frakes, L. A., et al., *Init. Repts. DSDP* 28: Washington (U.S. Govt. Printing Office), 437–513.

Clark, B. L., and Campbell, A. S., 1942. *Eocene Radiolarian Faunas from the Mt. Diablo Area, California.* Geol. Soc. Am. Spec. Paper 39.

Dinkelman, M. G., 1973. Radiolarian stratigraphy: Leg 16, Deep Sea Drilling Project. *In* van Andel, Tj. H., Heath, G. R., et al., *Init. Repts. DSDP,* 16: Washington (U.S. Govt. Printing Office), 747–813.

Ehrenberg, C. G., 1844. Uber 2 neue Lager von Gebirgsmassen aus Infusorien als Meeres-Absatz in Nord-Amerika und eine Vergleichung derselben mit den organischen Kreidegebilden in Europa und Afrika, *Abh. Kl. Preuss. Akad. Wiss. Berlin*, p. 57.

_____, 1858. Kurze Charakteristik der 9 neuen Genera und der 105 neuen Species des Agalischen Meers und des Tiefgrundes des Mittel-Meeres. *Monatsber. Kl. Preuss. Akad. Wiss. Berlin*, p. 10.

_____, 1873. Grossere Felsproben des Polycystinen-Mergels von Barbados mit weiteren Erlauterungen. *Monatsber. Kl. Preuss. Akad. Wiss. Berlin*, p. 213.

_____, 1875. Fortsetzung der mikrogeologischen Studien als Gesammt-Uebersicht der mikroskopischen Paläontologie gleichartig analysirter Gebirgsarten der Erde, mit spezieller Rucksicht auf den Polycystinen-Mergel von Barbados. *Abh. Kl. Akad. Wiss. Berlin*, pp. 1–226.

Foreman, H. P., 1973. Radiolaria of Leg 10 with systematics and ranges for the families *Amphipyndacidae, Artostrobiidae*, and *Theoperidae*. *In* Worzel, J. L., Bryant, W., et al., *Init. Repts. DSDP*, 10: Washington (U.S. Govt. Printing Office), 407–474.

_____, 1975. Radiolaria from the North Pacific, Deep Sea Drilling Project, Leg 32. *In* Larson, R. L., Moberly, R., et al., *Init. Repts. DSDP*, 32: Washington (U.S. Govt. Printing Office), 579–676.

Haeckel, E., 1887. *Report on the Scientific Results of the Voyage of H.M.S.* Challenger *during the Years 1873–1876. Zoology*, Vol. 18. *Report on the Radiolaria:* London (Eyre and Spottiswoode).

Haq, B. U., et al., 1980. Late Miocene marine carbon-isotopic shift and synchroneity of some phytoplanktonic biostratigraphic events. *Geology*, 8:427–431.

Hays, J. D., 1965. Radiolaria and late Tertiary and Quaternary history of Antarctic seas. *In* Llano, G. A. (Ed.), *Biology of the Antarctic Seas II.* Am. Geophys. Union, Antarct. Res. Ser., 5: 125–184.

Hays, J. D., Lozano, J. A., Shackleton, N., and Irving, G., 1976. Reconstruction of the Atlantic and western Indian Ocean sectors of the 18,000 B. P. Antarctic Ocean. *In* Cline, R. M., and Hays, J. D. (Eds.), *Investigation of Late Quaternary Paleoceanography and Paleoclimatology.* Geol. Soc. Am. Mem., 145:337–372.

Hays, J. D., and Opdyke, N. D., 1967. Antarctic radiolaria, magnetic reversals, and climatic change. *Science*, 158:1001–1011.

Hays, J. D., and Shackleton, N., 1976. Globally synchronous extinction of the radiolarian *Stylatractus universus. Geology*, 4: 649–652.

Johnson, D. A., 1974. Radiolaria from the eastern Indian Ocean, DSDP Leg 22. *In* von der Borch, C. C., and Sclater, J. G., et al., *Init. Repts. DSDP*, 22: Washington (U.S. Govt. Printing Office), 521–575.

Johnson, D. A., and Wick, B. J., 1982. Precision of correlation of radiolarian datum levels in the Middle Miocene, equatorial Pacific. *Micropaleontology*, 28:43–58.

Keany, J., 1979. Early Pliocene radiolarian taxonomy and biostratigraphy in the Antarctic region. *Micropaleontology*, 25:50–74.

Kellogg, D. E., 1975. The role of phyletic change in the evolution of *Pseudocubus vema* Radiolaria. *Paleobiology*, 1:359–370.

Kling, S. A., 1971. Radiolaria, Leg 6 of the Deep Sea Drilling Project. *In* Fischer, A. G., Heezen, B. C., et al., *Init. Repts. DSDP*, 6: Washington (U.S. Govt. Printing Office), 1069–1117.

_____, 1973. Radiolaria from the eastern North Pacific, Deep Sea Drilling Project, Leg 18. *In* Kulm, L. D., von Huene, R., et al., *Init. Repts. DSDP*, 18: Washington (U.S. Govt. Printing Office), 617–671.

Ling, H. Y., 1975. Radiolaria: Leg 31 of the Deep Sea Drilling Project. *In* Karig. D. E., Ingle, J. C., Jr., et al., *Init. Repts. DSDP*, 31: Washington (U.S. Govt. Printing Office), 703–761.

Lozano, J. A., and Hays, J. D., 1976. Relationship of radiolarian assemblages to sediment types and physical oceanography in the Atlantic and western Indian Ocean sectors of the Antarctic Ocean. *In* Cline, R. M., and Hays, J. D. (Eds.), *Investigation of Late Quaternary Paleoceanography and Paleoclimatology.* Geol. Soc. Am. Mem., 145:303–336.

Martin, G. C., 1904. Radiolaria. *Maryland Geol. Surv. (Miocene), Gen. Ser.*, pp. 447–459.

Moore, T. C. Jr., 1971. Radiolaria. *In* Tracey, J. I., Sutton, G. H., et al., *Init. Repts. DSDP*, 8: Washington (U.S. Govt. Printing Office), 727–775.

_____, 1972. Mid-Tertiary evolution of the radiolarian genus, *Calocycletta. Micropaleontology*, 18:244–252.

Moore, T. C., Jr., and Nigrini, C., 1979. *A Guide to Modern Radiolaria.* Cushman Found. Foram. Res. Spec. Publ. 16.

Nigrini, C., 1967. *Radiolaria in Pelagic Sediments from the Indian and Atlantic Oceans:* Berkeley and Los Angeles (Univ. California Press) Scripps Inst. Oceanogr. Bull. 11.

_____, 1977. Tropical Cenozoic Artostrobiidae (Radiolaria). *Micropaleontology*, 23:241–269.

Payne, R. D., 1977. Radiolaria in Brunhes sediments of the southeast Indian Ocean south of Australia [Ph.D. dissert.]. University of South Carolina, Columbia, S.C.

Petrushevskaya, M. G., 1968. Radiolarians of orders Spumellaria and Nasselaria of the Antarctic Region. *In* Andriiashev, A. P., and Ushakov, P. V. (Eds.), *Biological Reports of the Soviet Antarctic Expedition 1955–1958* (Vol. 3): Jerusalem (Israel Program for Scientific Translations), 2–186.

_____, 1975. Cenozoic radiolarians of the Antarctic, Leg 29, DSDP. *In* Kennett, J. P., Houtz, R. E., et al., *Init. Repts. DSDP*, 29: Washington (U.S. Govt. Printing Office), 541–675.

Petrushevskaya, M. G., and Kozlova, G., 1972. Radiolaria: Leg 14, Deep Sea Drilling Project. *In* Hays, D. E., Pimm, A. C., et al., *Init. Repts. DSDP*, 14: Washington (U.S. Govt. Printing Office), 495–648.

Riedel, W. R., 1957. Radiolaria: a preliminary stratigraphy. *Repts. Swedish Deep-Sea Exped. 1947–1948*, 6:61–96.

_____, 1958. Radiolaria in Antarctic sediments. *Repts. B.A.N.Z. Antarctic Res. Exped. Ser. B.*, 6:219–255.

_____, 1959. Oligocene and Miocene radiolaria in tropical Pacific sediments. *Micropaleontology*, 5:285–302.

Riedel, W. R., and Sanfilippo, A., 1970. Radiolaria, Leg 4, Deep Sea Drilling Project. *In* Bader, R. G., Gerard, R. D., et al., *Init. Repts. DSDP*, 4: Washington (U.S. Govt. Printing Office), 503–575.

_____, 1971. Cenozoic Radiolaria from the western tropical Pacific, Leg 7. *In* Winterer, E. L., Riedel, W. R., et al., *Init. Repts. DSDP*, 7: Washington (U.S. Govt. Printing Office), 1529–1672.

_____, 1977. Cenozoic Radiolaria. *In* A. T. S. Ramsey (Ed.), *Oceanic Micropaleontology:* New York (Academic Press), pp. 847–912.

_____, 1978. Stratigraphy and evolution of tropical Cenozoic radiolarians. *Micropaleontology*, 24:61–96.

Riedel, W. R., Sanfilippo, A., and Cita, M. B., 1974. Radiolarians from the stratotype Zanclean (Lower Pliocene, Sicily). *Riv. Ital. Paleont.*, 80:699–734.

Saito, T., Burckle, L. H., and Hays, J. D., 1975. Late Miocene to Pleistocene biostratigraphy of equatorial Pacific sediments. *In* Saito, T., and Burckle, L. H. (Eds.), *Late Neogene Epoch Boundaries:* New York (Micropaleontology Press, American Museum of Natural History), pp. 226–244.

Sanfilippo, A., and Riedel, W. R., 1970. Post-Eocene "closed" theoperid radiolarians. *Micropaleontology*, 16:446–462.

_____, 1973. Cenozoic radiolarians (exclusive of theoperids, artostrobiids, and amphipyndacids) from the Gulf of Mexico, Deep Sea Drilling Project Leg 10. *In* Worzel, J. L., Bryant, W., et al., *Init. Repts. DSDP*, 10: Washington (U.S. Govt. Printing Office), 475–611.

_____, 1980. A revised generic and suprageneric classification of the Artiscins (Radiolaria). *J. Paleontol.*, 54:1008–1011.

_____, 1982. Revision of the Radiolarian genera *Theocotyle, Theocotylissa,* and *Thyrsocyrtis. Micropaleontology*, 28:170–188.

Sanfilippo, A., Burckle, L. H., Martini, E., and Riedel, W. R., 1973. Radiolarians, diatoms, silicoflagellates, and calcareous nannofossils in the Mediterranean Neogene. *Micropaleontology*, 19: 205–234.

Weaver, F. M., 1976a. Antarctic radiolaria from the southeast Pacific Basin, DSDP, Leg 35. *In* Hollister, C. D., Craddock, C., et al., *Init. Repts. DSDP*, 35: Washington (U.S. Govt. Printing Office), 569–603.

_____, 1976b. Late Miocene and Pliocene radiolarian paleobiogeography and biostratigraphy of the Southern Ocean [Ph.D. dissert.]. Florida State University, Tallahassee.

Weaver, F. M., Casey, R. E., and Perez, A. M., 1981. Stratigraphic and paleoceanographic significance of early Pliocene to middle Miocene radiolarian assemblages from northern to Baja California. *The Monterey Formation and Related Siliceous Rocks of California.* Soc. Econ. Paleontol. Mineral. Spec. Publ., Pacific Sec., pp. 71–86.

Zachariasse, W. J., et al., 1978. Micropaleontological counting methods and techniques—an exercise on an eight metres section of the Lower Pliocene of Capo Rossello, Sicily. *Utrecht Micropaleontol. Bull.*, 17:81–128.

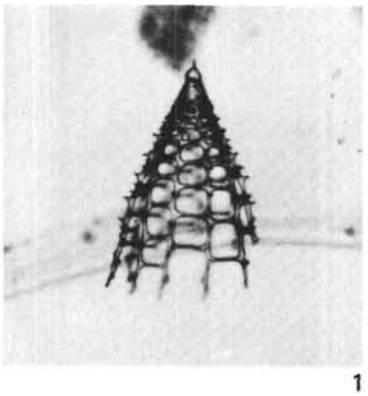

1

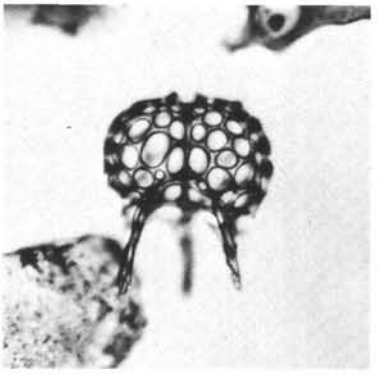

2

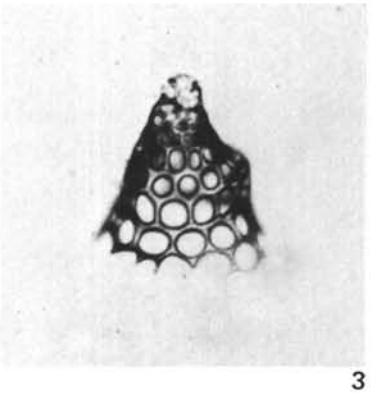

3

4

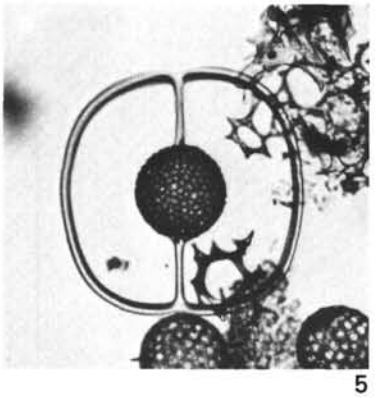

5

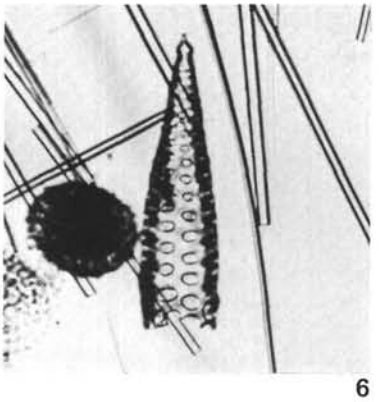

6

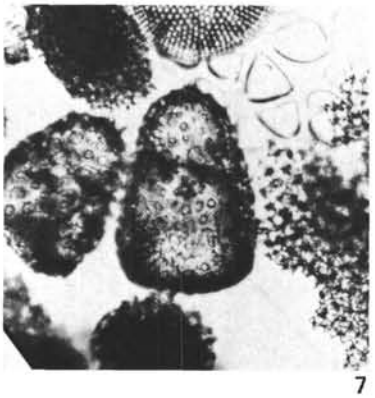

7

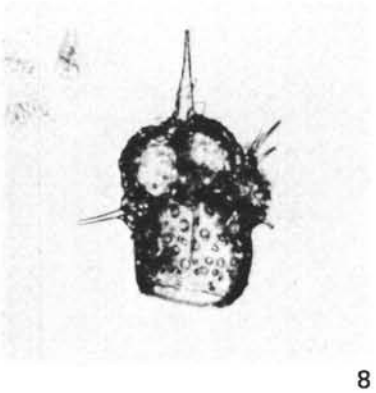

8

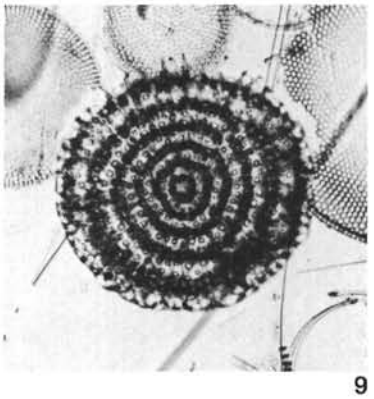

9

Plate 1. Cenozoic radiolarians. 1. *Peripyramis circumtexta*, ×140, Sample 513A-1-1, 137–139 cm. 2. *Triceraspyris antarctica*, ×200, Sample 324-1-4, 68–70 cm. 3. *Cycladophora davisiana*, ×250, Sample 324-1-1, 143–145 cm. 4. *Saccospyris antarctica*, ×240, Sample 324-1-1, 143–145 cm. 5. *Saturnalis circularis*, ×160, Sample 324-1-3, 82–84 cm. 6. *Cornutella profunda*, ×200, Sample 513A-1-1, 137–139 cm. 7. *Antarctissa denticulata*, ×200, Sample 514-4,CC. 8. *Saccospyris praeantarctica*, ×280, Sample 514-26,CC. 9. *Stylodictya validispina*, ×200, Sample 514-26,CC.

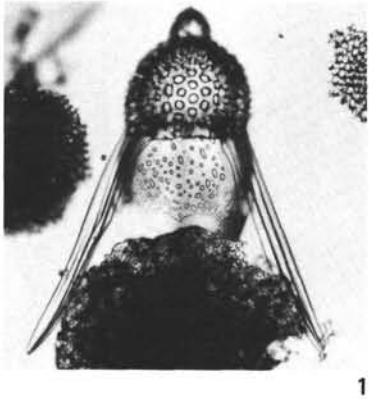
1

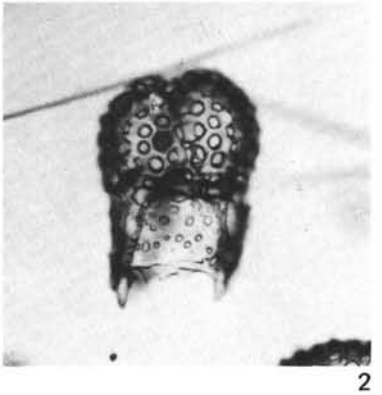
2

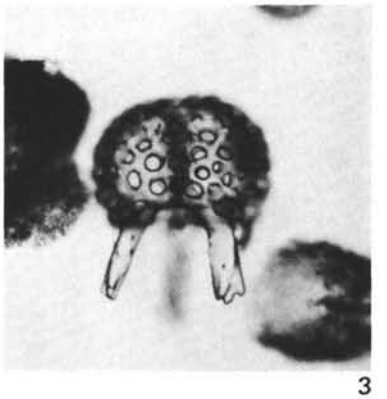
3


4


5

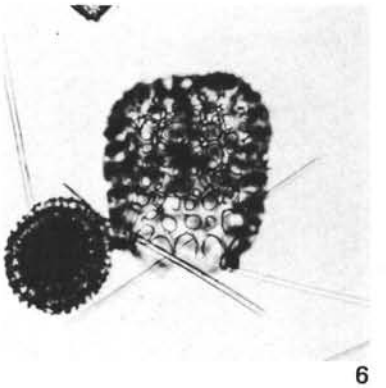
6

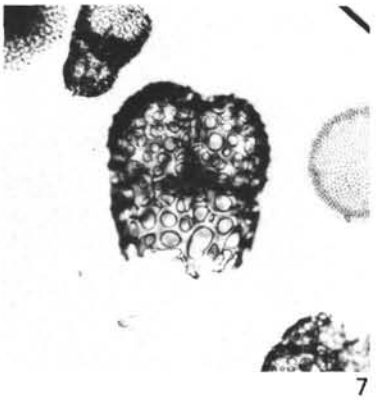
7

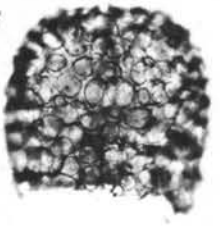
8

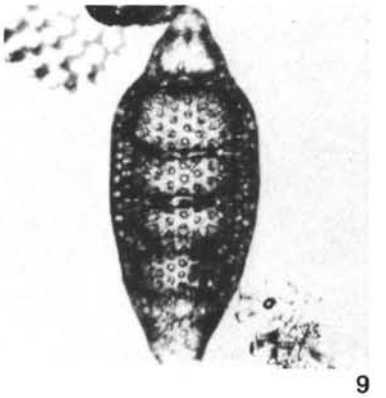
9

Plate 2. Cenozoic radiolarians. 1. *Lychnocanoma grande rugosum*, ×120, *Eltanin* Core 38–8, 460 cm. 2–3. *Triceraspyris coronata*, Sample 513A-3,CC, (2) ×195, (3) ×205. 4. *Theocorys redondoensis*, ×270, Sample 513A-5-4, 177–199 cm. 5. *Clathrocyclas bicornis*, ×200, Sample 513A-1,CC. 6–8. *Desmospyris spongiosa* (6–7) ×170, *Eltanin* Core 16–4(6, 220 cm; 7, 260 cm), (8) ×205, *Eltanin* Core 38–8, 280 cm. 9. *Eucyrtidium calvertense*, ×200, Sample 513A-1,CC.

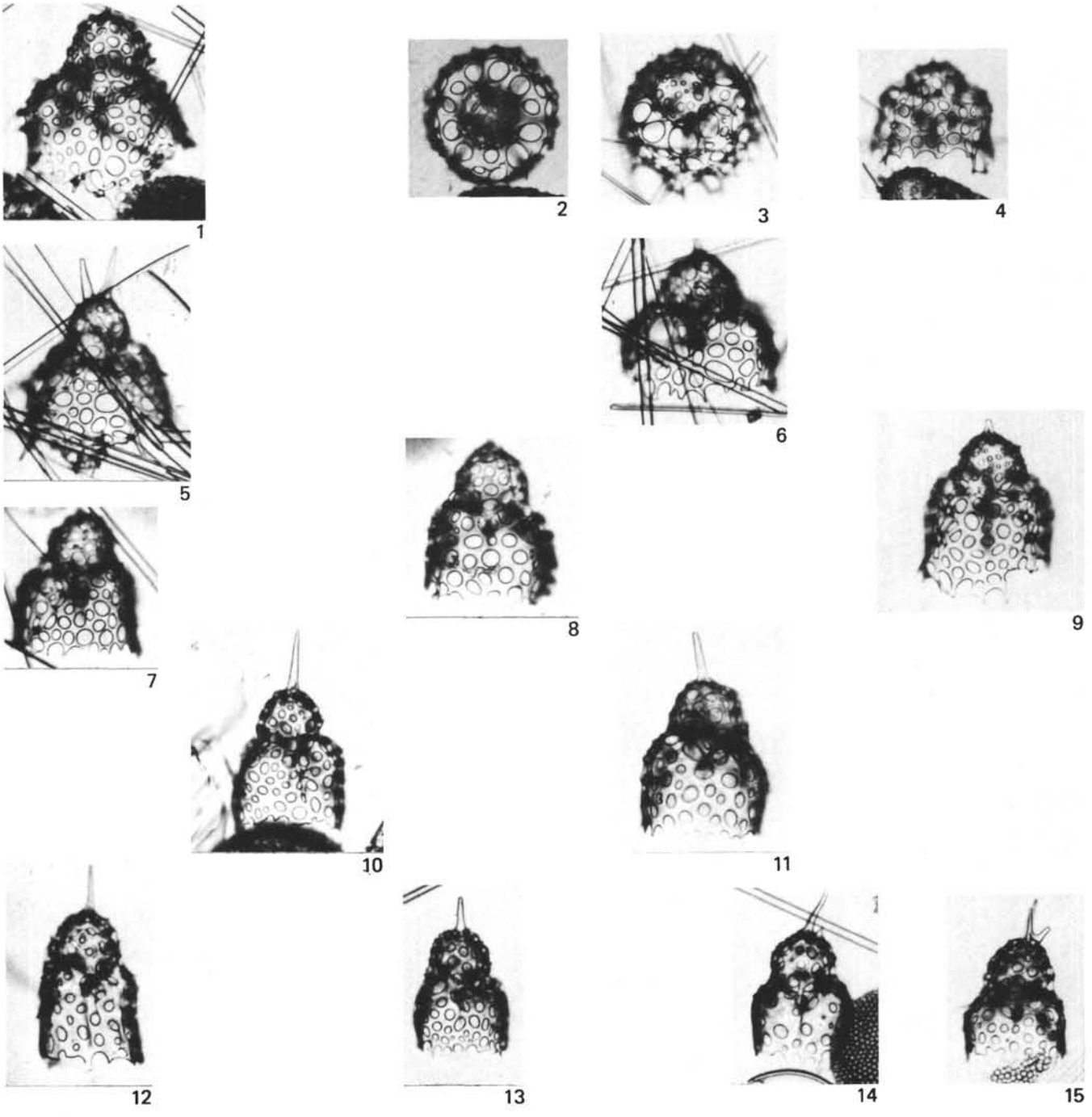

Plate 3. Cenozoic radiolarians. 1. *Helotholus praevema* n. sp., ×180, *Eltanin* Core 50–28, 380 cm. 2–4. *Helotholus vema*, (2–3) *Eltanin* Core 50–28, 380 cm. (2, ×155, plan view; 3, ×120), (4) ×135, *Eltanin* Core 38–8, 400 cm. 5–15. *Helotholus praevema*, (5–7) *Eltanin* Core 50–28 (5, 411 cm, ×170; 6, 380 cm, ×180, transitional form; 7, 300 cm, ×170), (8–10) *Eltanin* Core 38–8 (8, 460 cm, ×160; 9, 420 cm, ×165, holotype; 10, 460 cm, ×170), (11) *Eltanin* Core 34–17, 580 cm, ×175, (12–14) *Eltanin* Core 38–8 (12, 500 cm, ×175; 13, 520 cm, ×175; 14, 540 cm, ×170), (15) *Eltanin* Core 34–17, 592 cm, ×160.

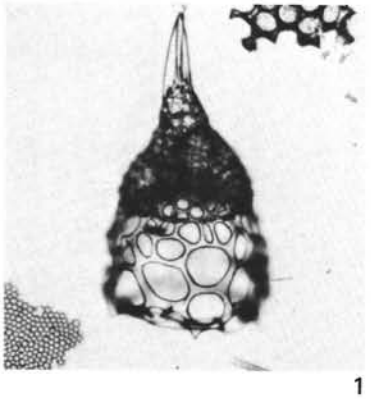

1

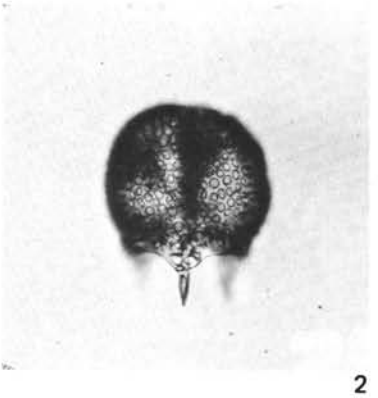

2

3

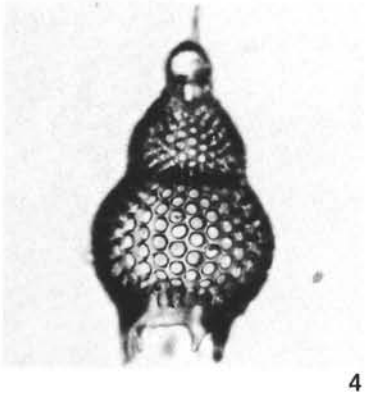

4

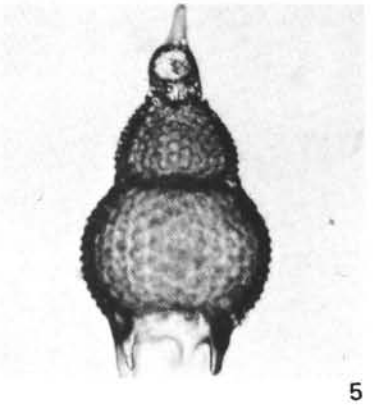

5

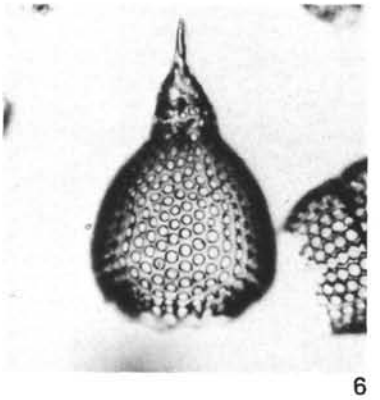

6

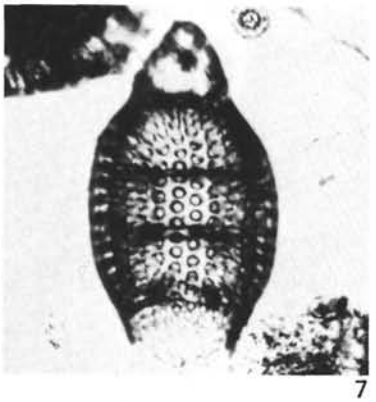

7

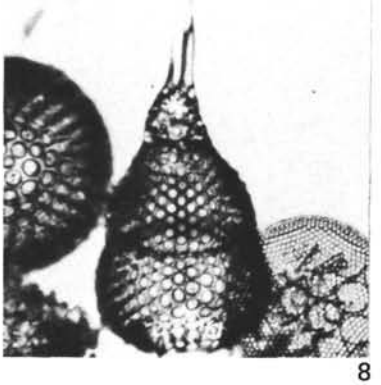

8

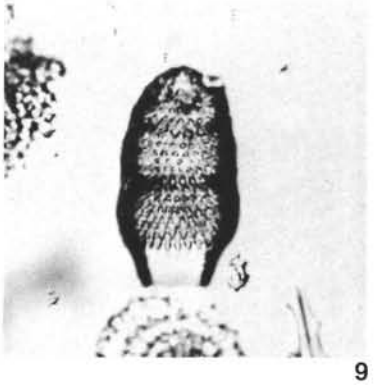

9

Plate 4. Cenozoic radiolarians. 1. *Lamprocyrtis heteroporos*, ×210, Sample 514-33,CC. 2–3. *Tholospyris* sp. A, ×200, Sample 514-33,CC. 4–5. *Lamprocyclas aegles* gp., ×170, Sample 513A-6-7, 33–35 cm. 6. *Anthocyrtidium ehrenbergii*, ×230, Sample 513A-7-2, 61–63 cm. 7. *Eucyrtidium calvertense* ×240, Sample 513A-1,CC. 8. *Lamprocyclas maritalis*, ×230, *Eltanin* Core 39–55, 691 cm. 9. *Siphocampe* sp. A, ×210, Sample 513A-6-5, 143–145 cm.

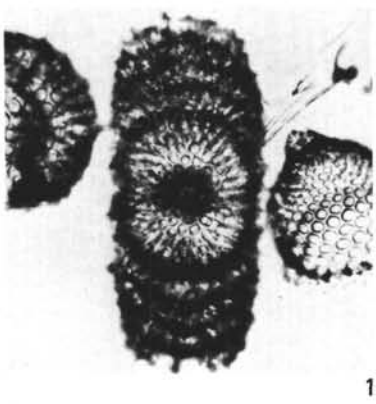
1

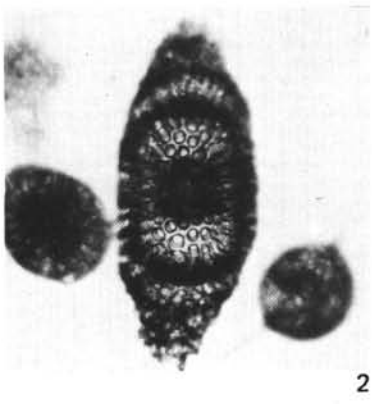
2

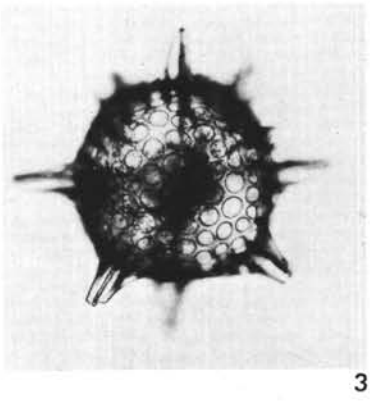
3

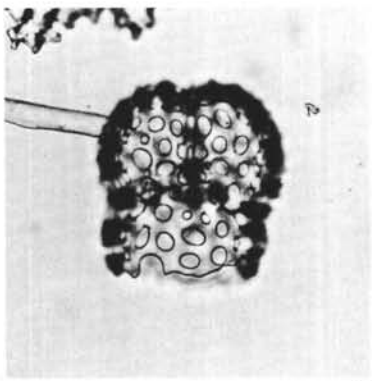
4


5

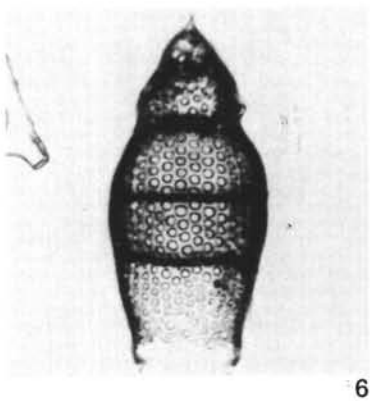
6


7

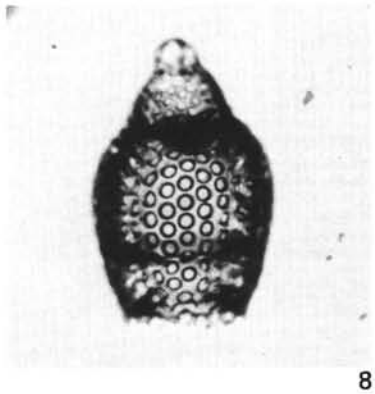
8

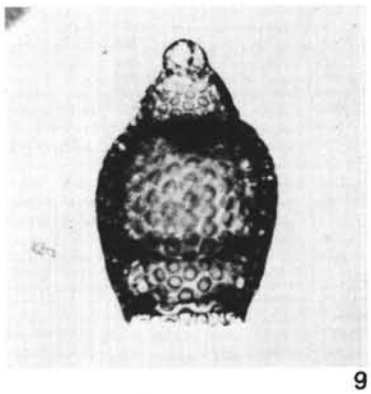
9

Plate 5. Cenozoic radiolarians. 1. *Diartus hughesi*, ×180, Sample 513A-10-5, 73–75 cm. 2. *Didymocyrtis antepenultimus*, ×175, Sample 266-11-1, 60–62 cm. 3. *Actinomma tanyacantha*, ×200, Sample 512-4-2, 58–60 cm. 4. *Dendrospyris haysi*, ×280, Sample 512-2,CC. 5. *Lithomelissa* sp. C, ×260, Sample 513A-10-4, 73–75 cm. 6. *Eucyrtidium cienkowskii* gp., ×220, Sample 513A-7-3, 143–145 cm. 7. *Theocalyptra bicornis spongothorax*, ×250, Sample 513A-10-4, 73–75 cm. 8–9. *Eucyrtidium pseudoinflatum* n. sp., ×285, Sample 278-10-5, 46–48 cm.

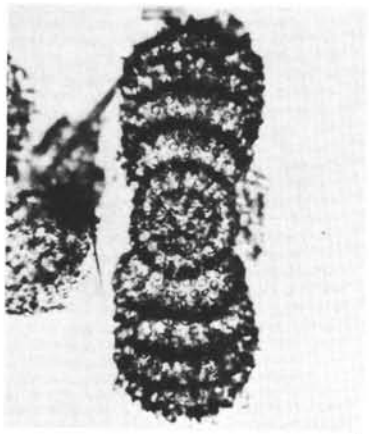

1

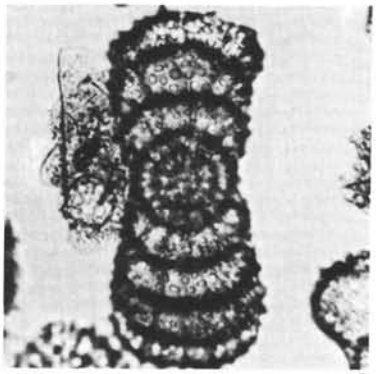

2

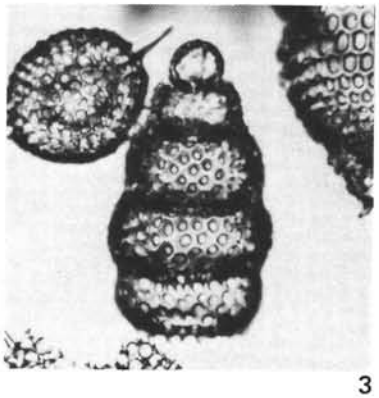

3

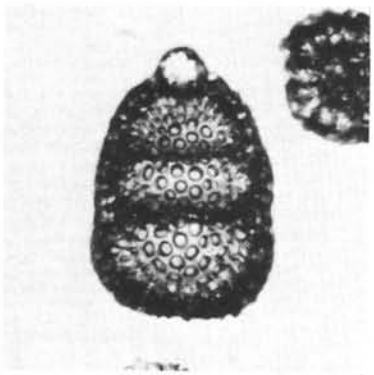

4

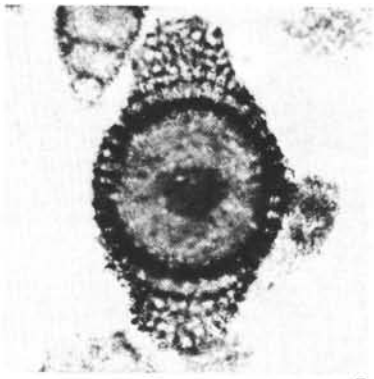

5

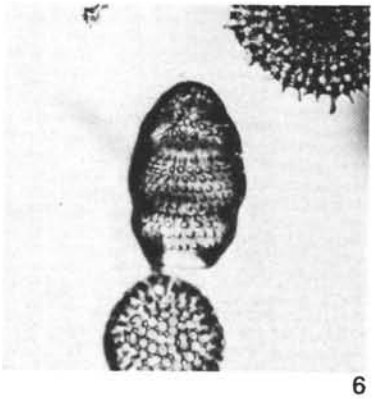

6

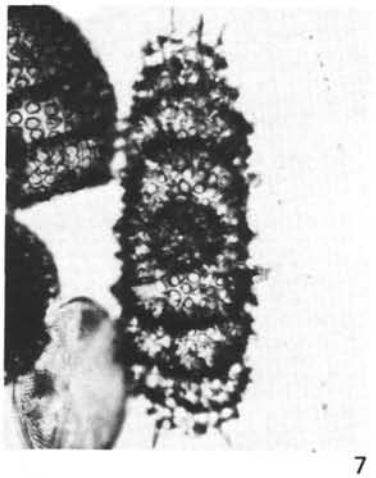

7

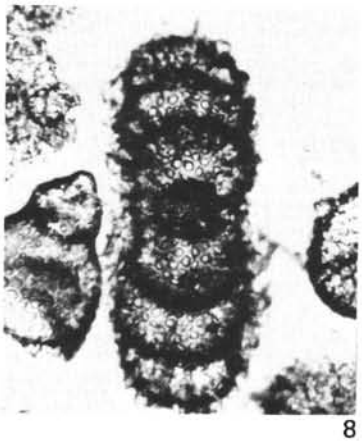

8

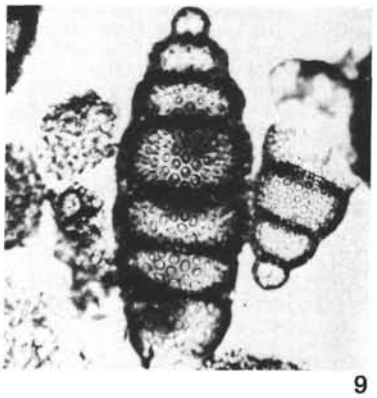

9

Plate 6. Cenozoic radiolarians. 1–2. *Amphymenium challengerae* n. sp., Sample 513A-5-7, 36–38 cm (1) ×230, holotype, (2) ×225. 3. *Stichocorys peregrina,* ×210, *Eltanin* Core 34–19, 80 cm. 4. *Cyrtocapsella tetrapera,* ×310, Sample 513A-11-3, 143–145 cm. 5. *Didymocyrtis* sp. A, ×160, Sample 513A-6-7, 33–35 cm. 6. *Siphocampe* sp. A, ×215, Sample 513A-6-5, 143–145 cm. 7–8. *Didymocyrtis didymus,* ×230, Sample 513A-6-3, 73–75 cm. 9. *Stichocorys peregrina,* ×180, Sample 513A-7-4, 143–145 cm.